

AD-A012 628

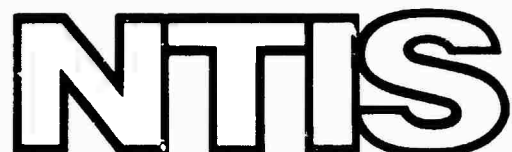
MODELING OMEGA PCA PHASE ADVANCES

P. E. Argo

Naval Electronics Laboratory Center  
San Diego, California

1 May 1975

DISTRIBUTED BY:



National Technical Information Service  
U. S. DEPARTMENT OF COMMERCE

ADA012628

NELC/TR 1960

212080

NELC/TR 1960

## MODELING OMEGA PCA PHASE ADVANCES

P. E. Argo  
Research and Development  
September 1974 through February 1975

1 May 1975

Prepared for  
Naval Air Systems Command (AIR 370)

D D C

JUL 24 1975

REF ID: A670760

D

APPROVED FOR PUBLIC RELEASE; DISTRIBUTION IS UNLIMITED

NAVAL ELECTRONICS LABORATORY CENTER  
SAN DIEGO, CALIFORNIA 92152

Reproduced by  
NATIONAL TECHNICAL  
INFORMATION SERVICE  
U.S. Department of Commerce  
Springfield, VA 22151

## UNCLASSIFIED

SECURITY CLASSIFICATION OF THIS PAGE (When Data Entered)

REPORT DOCUMENTATION PAGE		READ INSTRUCTIONS BEFORE COMPLETING FORM
1. REPORT NUMBER NELC Technical Report 1950 (TR 1950)	2. GOVT ACCESSION NO.	3. RECIPIENT'S CATALOG NUMBER
4. TITLE (and Subtitle)  MODELING OMEGA PCA PHASE ADVANCES		5. TYPE OF REPORT & PERIOD COVERED Research and Development Sept 1974 through Feb 1975
7. AUTHOR(s)  P. E. Argo		6. PERFORMING ORG. REPORT NUMBER
8. PERFORMING ORGANIZATION NAME AND ADDRESS  Naval Electronics Laboratory Center San Diego, CA 92152		10. PROGRAM ELEMENT, PROJECT, TASK AREA & WORK UNIT NUMBERS  NELC M207
11. CONTROLLING OFFICE NAME AND ADDRESS  Naval Electronics Laboratory Center San Diego, CA 92152		12. REPORT DATE 1 May 1975
14. MONITORING AGENCY NAME & ADDRESS (if different from Controlling Office)  Naval Air Systems Command (A)R 370 Washington, DC		13. NUMBER OF PAGES 38
16. DISTRIBUTION STATEMENT (of this Report)  Approved for public release; distribution is unlimited		15. SECURITY CLASS. (of this report)  UNCLASSIFIED
		15a. DECLASSIFICATION/OWNGRADING SCHEDULE N/A
17. DISTRIBUTION STATEMENT (of the abstract entered in Block 20, if different from Report)  D D C JUL 24 1975 REF ID: A621762 D		
18. SUPPLEMENTARY NOTES		
19. KEY WORDS (Continue on reverse side if necessary and identify by block number)  Solar flares, propagation ducts, VLF radio transmission, electron particles, propagation phase advances, geomagnetic influences.		
20. ABSTRACT (Continue on reverse side if necessary and identify by block number)  The ejection of large numbers of protons (and other charged particles) as a result of solar flares and their direction into the polar ionosphere effectively lowers the reflection height for vlf propagation. Two paths in the polar region were studied and were found to be altered significantly by solar-flare activity. Additional paths in the polar region should be investigated to determine the existence of an enhanced D-region and its effect upon navigational systems.		

## **SUMMARY**

### **PROBLEM**

The ejection by solar flares of large numbers of protons (and other charged particles) and their direction into the polar ionosphere by the geomagnetic field, effectively lowers the reflection height for vlf propagation. A study of these effects was made using vlf data obtained in a high altitude investigation in Alaska during the period between May 1969 and November 1970.

### **RESULTS**

Analysis of the data obtained during the Alaska investigation, together with previously published information on the relation of phase advances due to solar protons and proton flux data obtained from Explorer 41, allowed the development of an empirical model which was used to reduce phase errors of the Omega navigational system to within 10 centicycles. This made it possible to reduce navigational errors in the Omega system from greater than 10 nautical miles to less than one nautical mile.

### **RECOMMENDATIONS**

Additional propagation paths in the polar region should be investigated in order to determine the existence of an extra enhanced D-region corresponding to the auroral oval. Knowledge of such a propagation structure would be very important to the prediction of the behavior of propagation paths crossing the low-altitude extremities of the polar cap and would enable the Omega system to warn navigators of the existence of propagation phase errors and would increase the navigational accuracy of the system.

### **ADMINISTRATIVE INFORMATION**

This study was made for the Naval Air Systems Command (AIR 370) by the Naval Electronics Laboratory Center, Propagation Technology Division, Code 2200, under project M207, as part of an effort to develop earth environment disturbance forecasting techniques. The author appreciates the technical discussions and manuscript review by Dr. I. J. Rothmiller and Mr. J. Hill. This work was performed between September 1974 and February 1975.

## CONTENTS

INTRODUCTION . . . page 5

ANALYSIS . . . 5

    Undisturbed Diurnal and Seasonal Phase Variations . . . 5  
    PCA Phase Advance Models . . . 8

DATA DESCRIPTION . . . 12

DISCUSSION . . . 29

    Latitudinal Extent of the Polar Cap . . . 30  
    Determination of Altitude Structure of Effective Loss Rate . . . 32

SUMMARY . . . 34

REFERENCES . . . 37

## ILLUSTRATIONS

1. Monthly average phase versus real-day phase . . . page 6
2. Single seasonal model . . . 7
3. Diurnal variation versus path in sunlight . . . 8
4. Diurnal patterns and phase variations . . . 9
5. Diurnal variations as changes in slope of  $\Delta\phi$  versus log-log (10f) relationships . . . 10
6. Diurnal variations predicted by weighted averaging . . . 11
7. PCA events, 25, 26, 27, 28 and 29 September 1969 . . . 13
8. PCA events, 14 and 15 October 1969 . . . 14
9. PCA events, 2, 3, 4 and 5 November 1969 . . . 15
10. PCA events, 24 and 25 November 1969 . . . 16
11. PCA events, 18, 19, 20, 21 and 22 December 1969 . . . 17
12. PCA events, 30 and 31 December 1969 . . . 18
13. PCA events, 28, 29, 30 and 31 January 1970 and 1 February 1970 . . . 19
14. PCA events, 6, 7, 8, 9 and 10 March 1970 . . . 20
15. PCA events, 23, 24, 25, 26 and 27 March 1970 . . . 21
16. PCA events, 28, 29, 30 and 31 March 1970 and 1 April 1970 . . . 22
17. PCA events, 5, 6 and 7 May 1970 . . . 23
18. PCA events, 30 and 31 May 1970 and 1, 2 and 3 June 1970 . . . 24
19. PCA events, 13, 14, 15, 16 and 17 June 1970 . . . 25
20. PCA events, 25, 26, 27, 28 and 29 June 1970 . . . 26
21. PCA events, 7, 8 and 9 July 1970 . . . 27
22. PCA events, 21, 22, 23, 24 and 25 July 1970 . . . 28
23. Corrected geomagnetic altitude, New York-to-Wales path . . . 31
24. VLF polar cap boundary . . . 31
25. Ionization rate . . . 33
26. Measured phase advance . . . 33

## **ILLUSTRATIONS (Continued)**

27. Reflected electron density . . . page 33
28. Effective electron-loss rate . . . 34
29. PCA event using Liberian station . . . 35
30. PCA event using Trinidad station . . . 36
31. Before and after positioning errors during a severe event . . . 36

## **TABLE**

1. Propagation Models . . . page 12

## INTRODUCTION

It has been known for many years that some solar flares eject large numbers of protons (and other charged particles) and that the geomagnetic field directs these particles into the polar atmosphere. These solar protons increase the ionization in the polar D-region, causing increased electron densities at altitudes from 40 to 80 kilometers. These increased densities effectively lower the "reflection height" for vlf propagation.

Assuming long-path conditions, at the low Omega frequencies (10.2 and 13.6 kHz) single-mode propagation is in effect and the lowered reflection height results in phase advances. Recently, Westerlund<sup>1</sup> observed that the maximum phase advance of a transpolar vlf signal was proportional to the log of the proton flux ( $> 10$  MeV).

In this report, an empirical model is presented which relates vlf phase advances to incident proton flux. This model uses the vlf data obtained in a high-latitude propagation study by the Naval Electronics Laboratory Center (NELC) in Alaska during the period from May 1969 to September 1970. The model also uses information on phase advances due to solar protons for 15 events previously reported by Martin.<sup>2</sup> Proton flux data was obtained from Explorer 41. The empirical model deduced from these data can be used to reduce Omega phase errors to within 10 centicycles which, in turn, reduces navigational errors from greater than 10 nautical miles to less than one nautical mile.

At the present time, the Omega system does not have the capability of warning navigators of phase errors caused by solar disturbances (or even of warning that an error-causing event is in progress). Future modifications to the Omega system should include these extended error-correcting modeling capabilities.

## ANALYSIS

### UNDISTURBED DIURNAL AND SEASONAL PHASE VARIATIONS

The undisturbed phase variations need to be accurately modeled because the disturbance phase advances are determined by the difference between the measured phase and the usual undisturbed phase.

The major phase variations are diurnal. During daylight hours, the phase is advanced relative to the nighttime. These diurnal variations are solar-caused because the D-region is formed basically by solar X-ray and Lyman-alpha ionization. VLF radio signals are reflected in the D-region.

Initially, the monthly average phase (at each hour) was expected to be close to the undisturbed phase. During the summer and winter months, this is almost the case. But, during the equinoxes, the sunlight conditions change rapidly (relative to a one-month period) and the monthly average may not correspond to any real day whatsoever. This effect is illustrated in figure 1.

The Omega system has developed an extensive "skywave" correction scheme to allow accurate estimates to be made of the expected phase. However, in this study, a simpler method has been developed. The diurnal variations of each path were modeled by using

---

1. Westerlund, S., F. H. Reder, and C. Asom, "Effects of Polar Cap Absorption Events on VLF Transmissions," Planet, Space Science, Vol. 17, p. 1329, 1969.

2. Martin, J. N., Omega Phase Variations During PCA Events, NELC TR 1835, 17 August 1972.

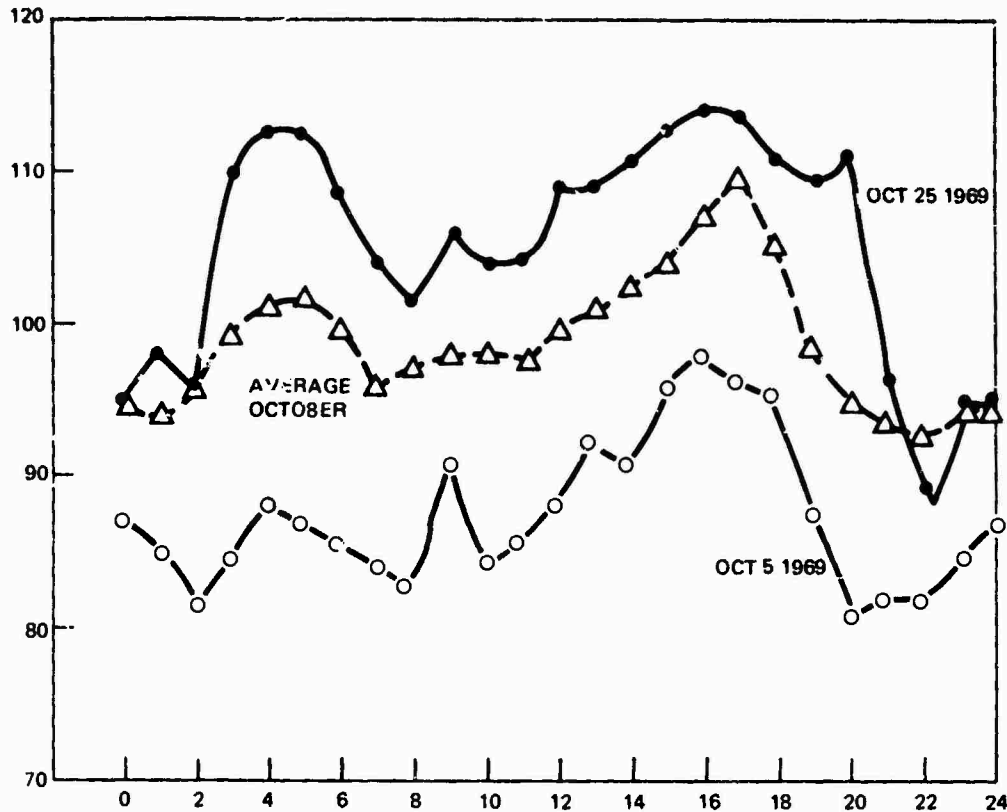


Figure 1. Monthly average phase versus real-day phase.

only that portion of the path which was in sunlight. Indeed, a single model is good for all seasons (as shown in figure 2), indicating that the seasonal effects on the diurnal variations are almost completely due to the varying amounts of the path in sunlight. The amount of sunlit path (for the two paths reported upon) may vary from zero to 50 percent during the winter, from 50 percent to 100 percent during the summer, and from zero to 100 percent in the spring and fall months.

The diurnal phase variations appear complex often with apparent 12-hour periods. These variations are immediately explained by examining the diurnal variations in the amount of path in sunlight, as shown in figure 3. This 12-hour period is seen on paths which lie near the North Pole and is caused by alternating ends of the path being in sunlight.

The unexpected fact that the phase variations are almost completely explained by the fraction of the path being in sunlight indicates that the undisturbed D-region seasonal chemistry changes (increased summer-loss rates)<sup>3, 4, 5</sup> are offset by some other factors. All that is determined in this report is that the quiet-time vlf reflection height is a function only of the day-night conditions.

- 
3. Montbriand, L. E., and J. S. Belrose, "Effective Electron Loss Rates in the Lower D-Region During the Decay of Solar X-Ray Events," Radio Science, Vol. 7, No. 1, p 133-172, 1972.
  4. Larsen, T. R., Disturbances in the High Latitude Lower Ionosphere, NDRE Report 62, Norwegian Defense Research Establishment, March 1973.
  5. Argo, P. E., and I. J. Rothmuller, Effective Electron Loss Rates in the Polar D-Region During Polar Cap Absorption Events, NELC TN 2890, 18 February 1975.

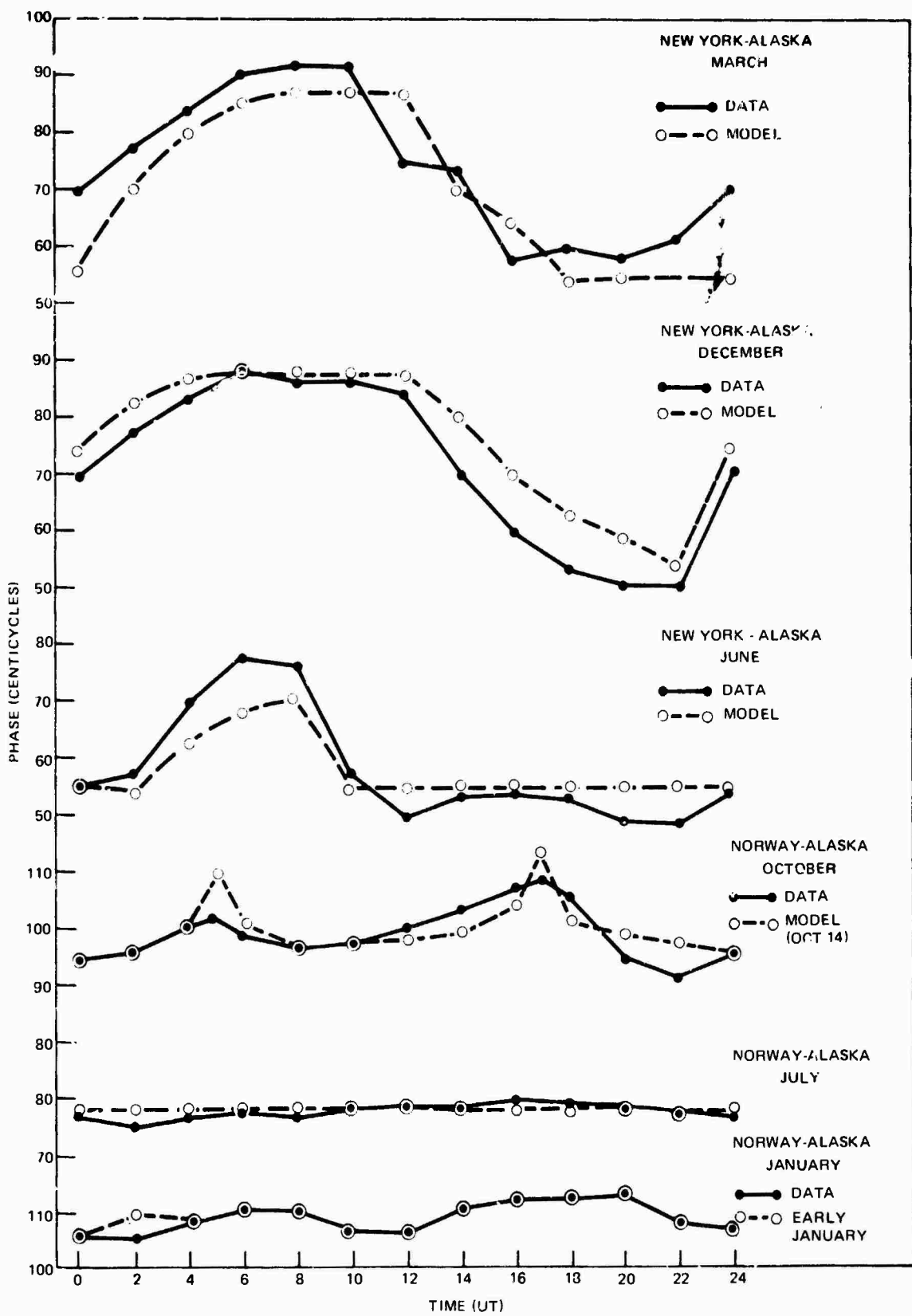


Figure 2. Single seasonal model.

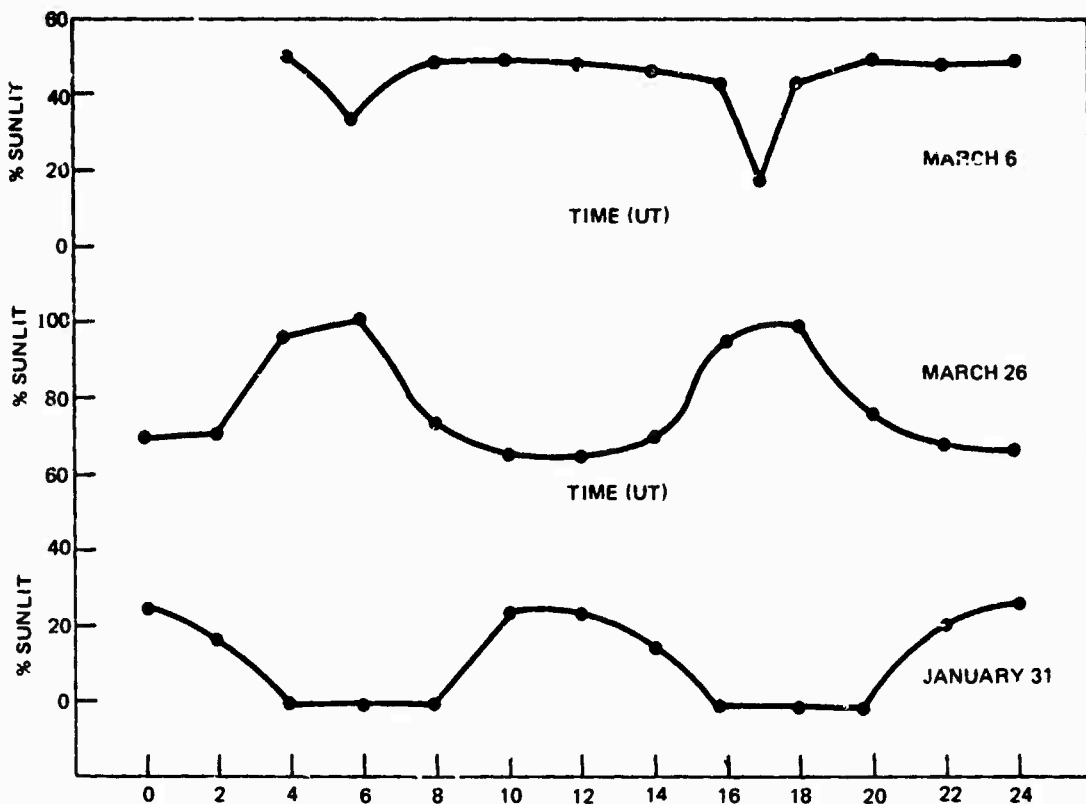


Figure 3. Diurnal variation versus path in sunlight.

#### PCA PHASE ADVANCE MODELS

Once the polar cap absorption (PCA) disturbance phase advances ( $\Delta\phi$  = measured phase minus the normal undisturbed phase) were determined, a regression fit to log-log (10 flux ( $>10$  MeV)) was used to generate a first-order model to the PCA variations. The factor of 10 in the log-log term was chosen to give a needed expansion in the flux axis. Another factor might be equally suitable.

Although the basic shape of the calculated phase-advance curve was similar to measurements, a distinct diurnal pattern was observed. This is shown in figure 4a. New regression fits, using only total-day and total-night data, yielded an envelope to the phase variations as shown in figure 4b. The model was constrained to give zero phase advance for some minimum flux ( $0.3 \text{ protons cm}^{-2} \text{ st}^{-1} \text{ sec}^{-1}$ ) under all diurnal conditions. These diurnal variations are fitted as changes in the slope of the  $\Delta\phi$  versus log-log (10f) relationship in figure 5. This fit is reasonable because the quiet model was developed to describe diurnal variations where the usual "quiet" flux is approximately  $0.3 \text{ protons cm}^{-2} \text{ st}^{-1} \text{ sec}^{-1}$ . The two paths showed distinct seasonal variations with the winter day being much more sensitive to changes in proton flux than the summer day.

The phase advances versus log-log (10f) for the Norway-to-Alaska path are plotted for three different conditions in figure 5: summer day (100 percent of the path in sunlight), spring and fall day (100 percent of the path in sunlight), and winter night (zero percent of the path in sunlight). During the summer, the Norway-to-Alaska path is always at least

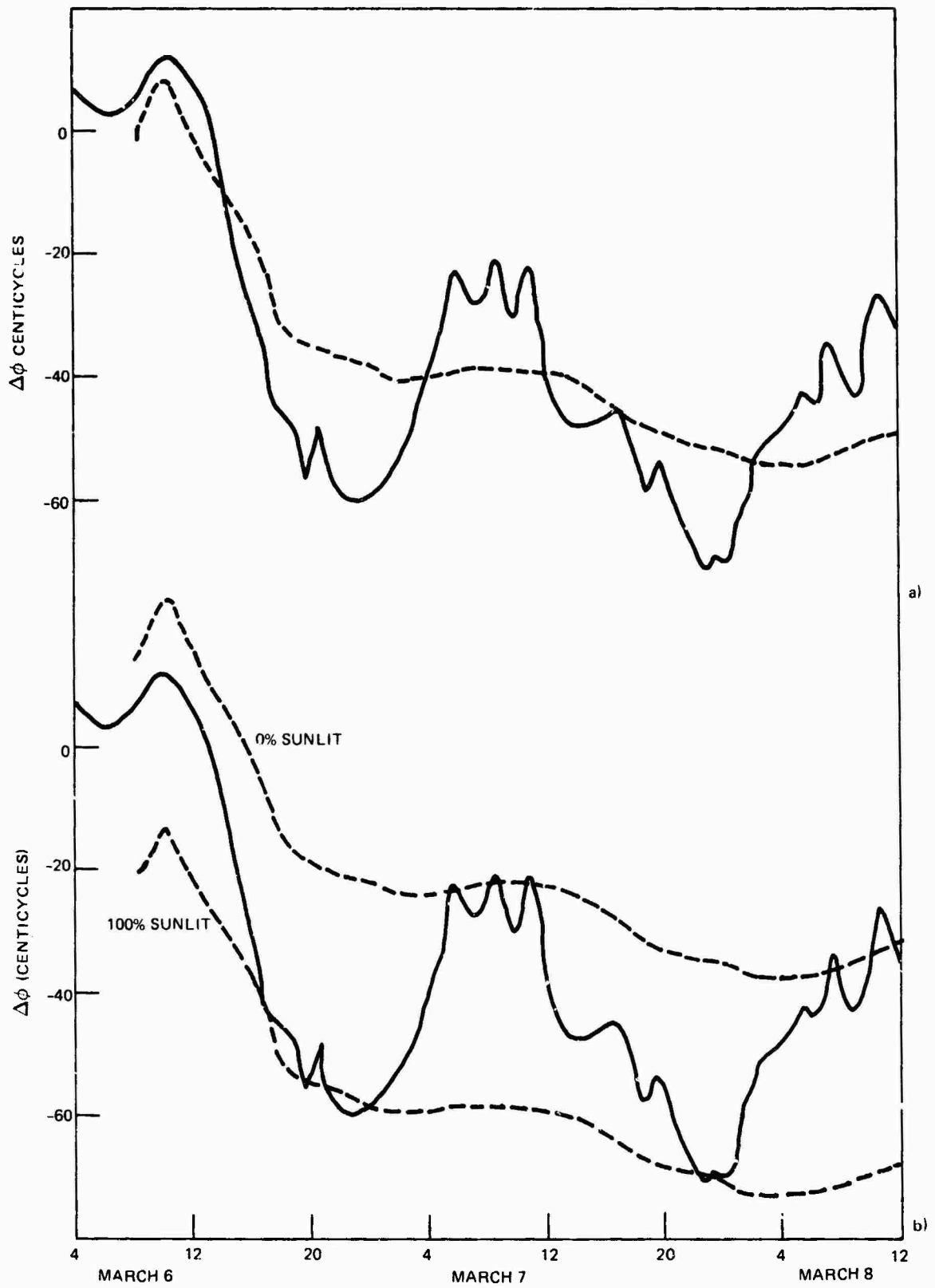


Figure 4. Diurnal patterns and phase variations.

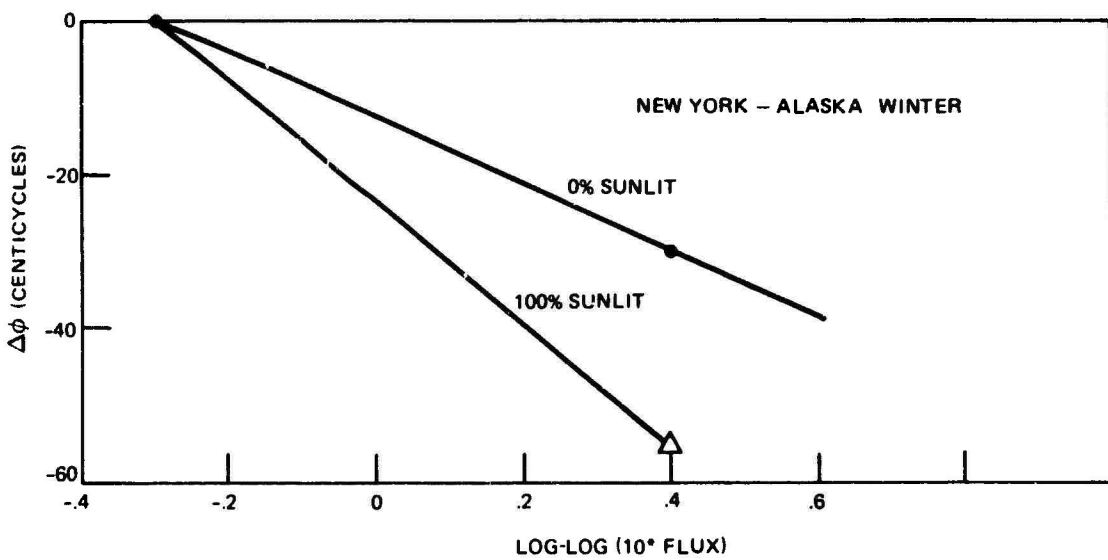


Figure 4. (Continued)

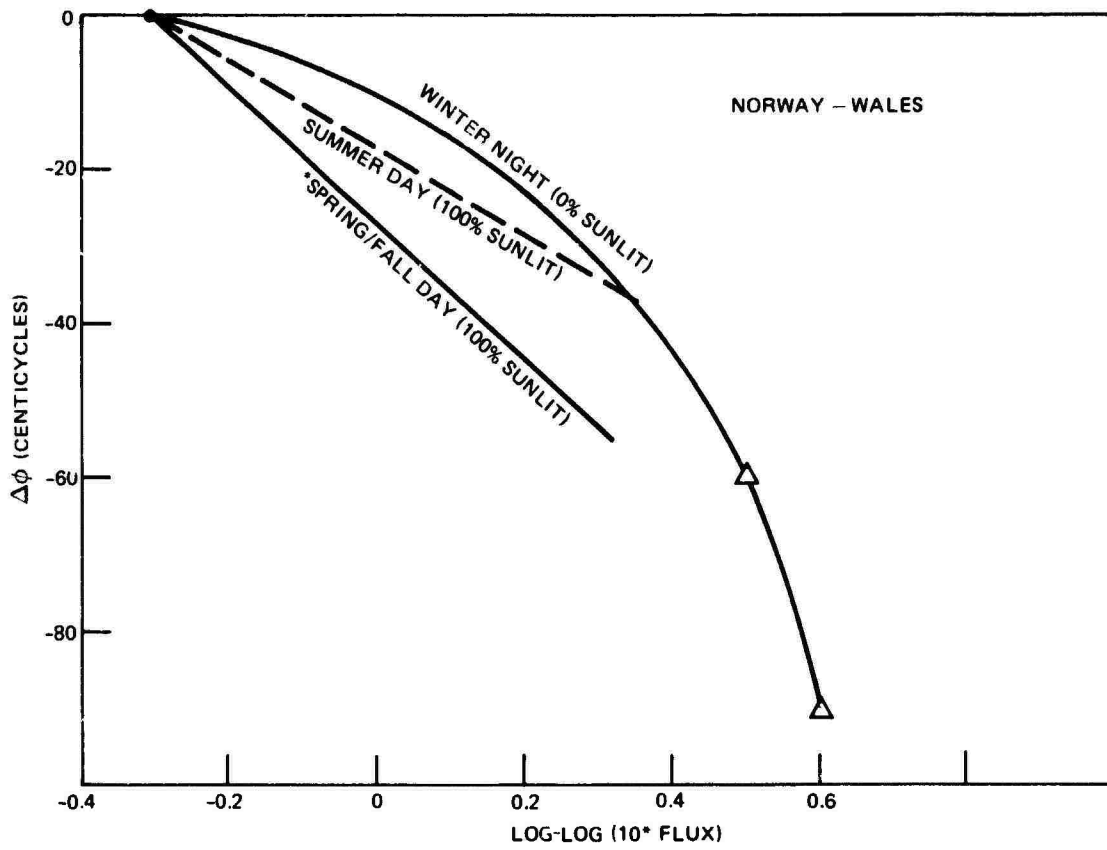


Figure 5. Diurnal variations as changes in slope of  $\Delta\phi$  versus log-log ( $10f$ ) relationships.

partially sunlit while, during the winter, the path is never totally sunlit. The spring-fall periods are more complex. Extrapolating the 100 percent and 50 percent sunlit spring-fall data to zero percent sunlit conditions, results in a phase advance (zero percent sunlit) versus proton-flux curve that approximates the winter zero-percent sunlit data. For this reason, the three seasons were combined into one model. For the Norway-to-Alaska path, a complete diurnal model was developed for the fall-winter-spring seasons. The Norway summer path is always sunlit 100 percent of the time, and so no estimate of the summer nighttime phases could be made.

Except for summer, the New York-to-Alaska path has conditions in which there is sunlight ranging from zero to 100 percent for most of the year. This complete range of variation enabled the development of a complete diurnal model having the fall-spring model merged with the winter model for this path. The summer-day (100 percent sunlit) and the spring-fall day (100 percent sunlit) phase advances were best fit by a linear relationship to log-log (10f) for the range of proton fluxes which were observed. However, the extremely large event of 2 November 1960 produced a nonlinear phase advance versus log-log (10f) relationship for the winter night. The summer and spring-fall paths may also respond in a nonlinear manner during events larger than those observed during the corresponding period. To simplify the winter model, two straight lines were fitted to the curves. Diurnal variations are predicted by weighted averaging of the measured (zero percent) and deduced (100 percent) sunlit curves and are shown in figure 6.

Table 1 contains the models for the New York-to-Alaska and Norway-to-Alaska paths for summer and winter (spring-fall) conditions and diurnal variations. These models provide an accurate fit to the measured phase advances for the fifteen available events.

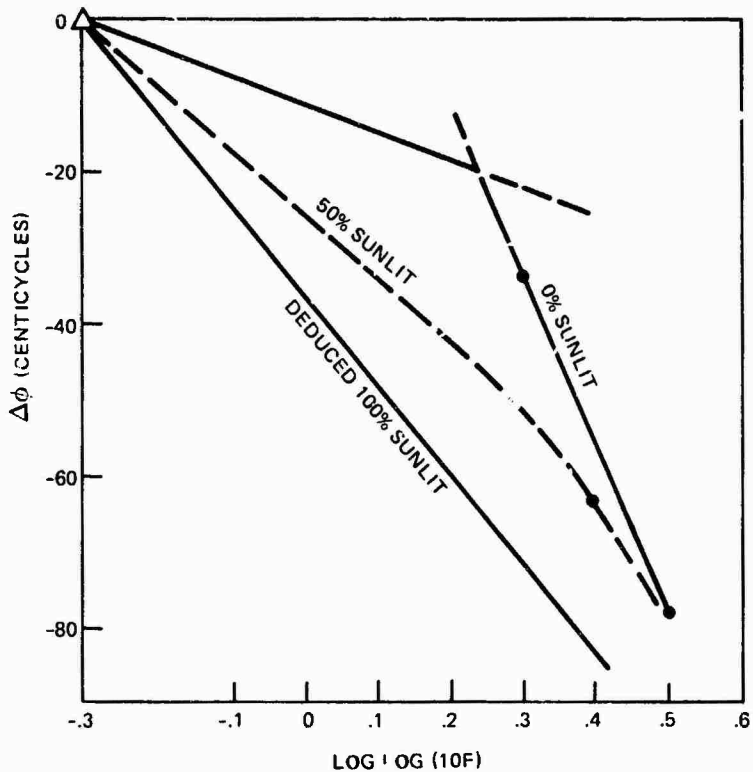


Figure 6. Diurnal variations predicted by weighted averaging

TABLE I. PROPAGATION MODELS.

**Norway-Alaska**

Summer:

$$\Delta\phi = [\log \log (10f) + 0.3] [-20. - 0.33 * \% \text{ sunlit}]$$

model error,  $\sigma = 3.6$  centicycles

Winter:

$$\Delta\phi = -[\log \log (10f) + 0.3] * 1.05 * \% \text{ sunlit} - XNIGHT * [1 - 0.01 * \% \text{ sunlit}]$$

$$XNIGHT = \begin{cases} [\log \log (10f) + 0.3] * 33 & \text{if } \log \log (10f) < 2 \\ [\log \log (10f) - 0.1] * 170 & \text{if } \log \log (10f) \geq 2 \end{cases}$$

model error,  $\sigma = 8.8$  centicycles

**New York-Alaska**

Summer:

$$\Delta\phi = [\log \log (10f) + 0.3] * [-20. - 0.20 * \% \text{ sunlit}]$$

model error,  $\sigma = 9.96$  centicycles

Winter:

$$\Delta\phi = [\log \log (10f) + 0.3] * [-37. - 0.43 * \% \text{ sunlit}]$$

model error  $\sigma = 9.0$  centicycles

## DATA DESCRIPTION

In this section, the individual events used in this study will be examined. Figures 7 through 22 include all of these events and contain the measured and modeled phase advances. The 25 September 1969 event has a double peak in the proton flux (one on 25 September and another on 28 September.) Both show up in the Omega phase data.

The 2 November 1969 event was the largest in the data set. The proton flux ( $> 10$  MeV) exceeded  $10^3 \text{ ster}^{-1} \text{ cm}^{-2} \text{ sec}^{-1}$ , while the next largest event had a proton flux ( $> 10$  MeV) of  $10^2$ . Notice the differences in the phase advances caused by path conditions (sunlight variations). The Norway path never has more than 25 percent of the path in sunlight while the New York path was modulated by zero to 100 percent of the path being in sunlight.

The 30 December 1969 event was very small. The proton flux never exceeded  $2 \text{ ster}^{-1} \text{ cm}^{-2} \text{ sec}^{-1}$ , with phase advances in the 10-to-15 centicycle regime. The Norway path was undergoing a strange, unexplained phase retardation during the event and so the modeled advances have the correct shape but are shifted by  $\sim 10$  centicycles.

During the 28 January 1970 event, the Norway to Alaska path had a variation in sunlight between zero and 25 percent while the New York to Alaska path underwent changes of from zero to 100 percent. The Norway path (which has almost no diurnal variations) shows the triple-peak structure in the solar proton flux (peaks at 0000 hours UT on 30 January and 0000 hours UT on 1 February). The New York path has diurnal variations which almost equal the proton flux effects.

The 6 March 1970 event was the first in the set to have a geomagnetic sudden commencement (SC) during the phase advance. According to some models of PCAs, there should be an expansion toward the equator at the time of the SC. This would show up as

(text resumes on p 29)

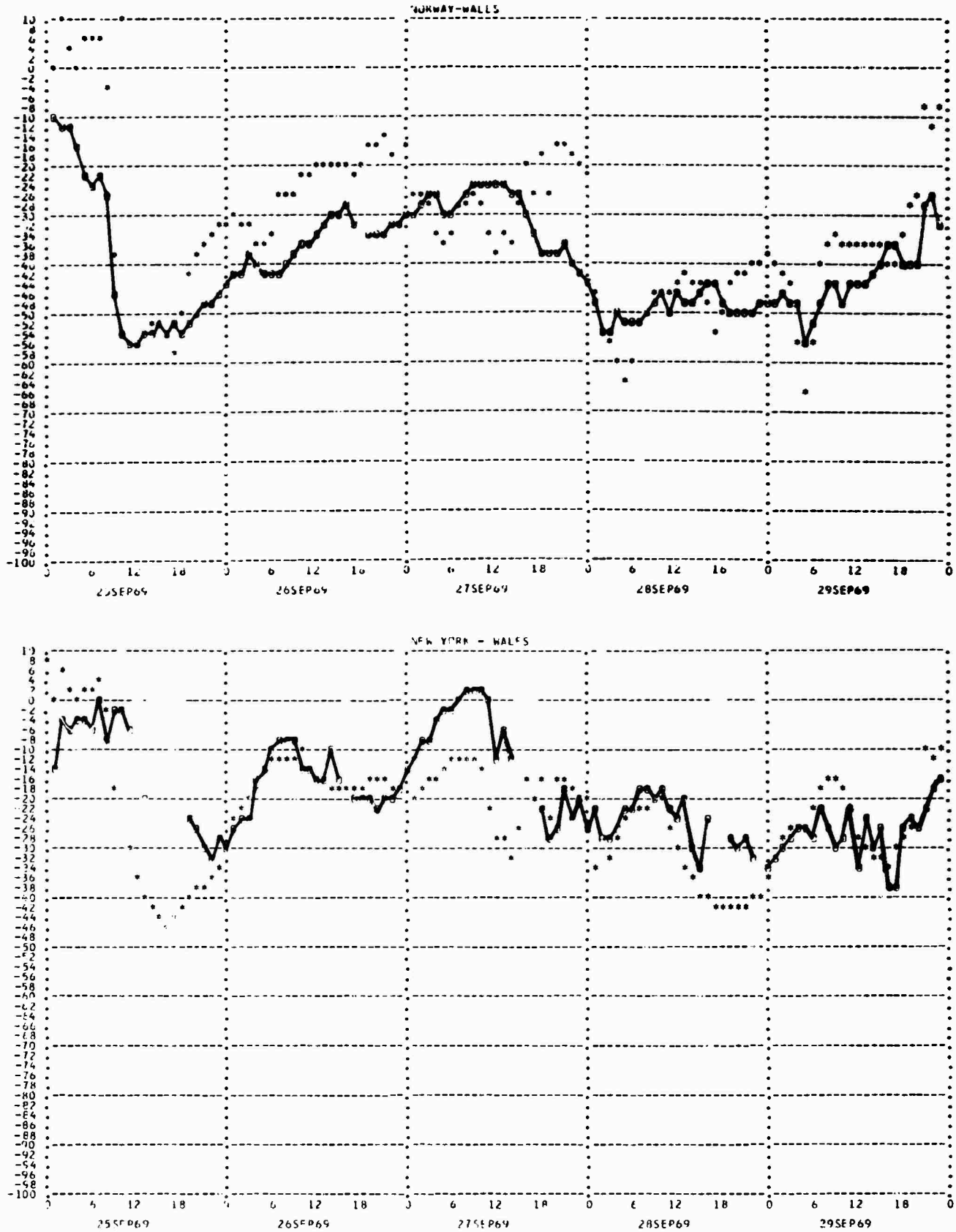


Figure 7. PCA events, 25, 26, 27, 28 and 29 September 1969.

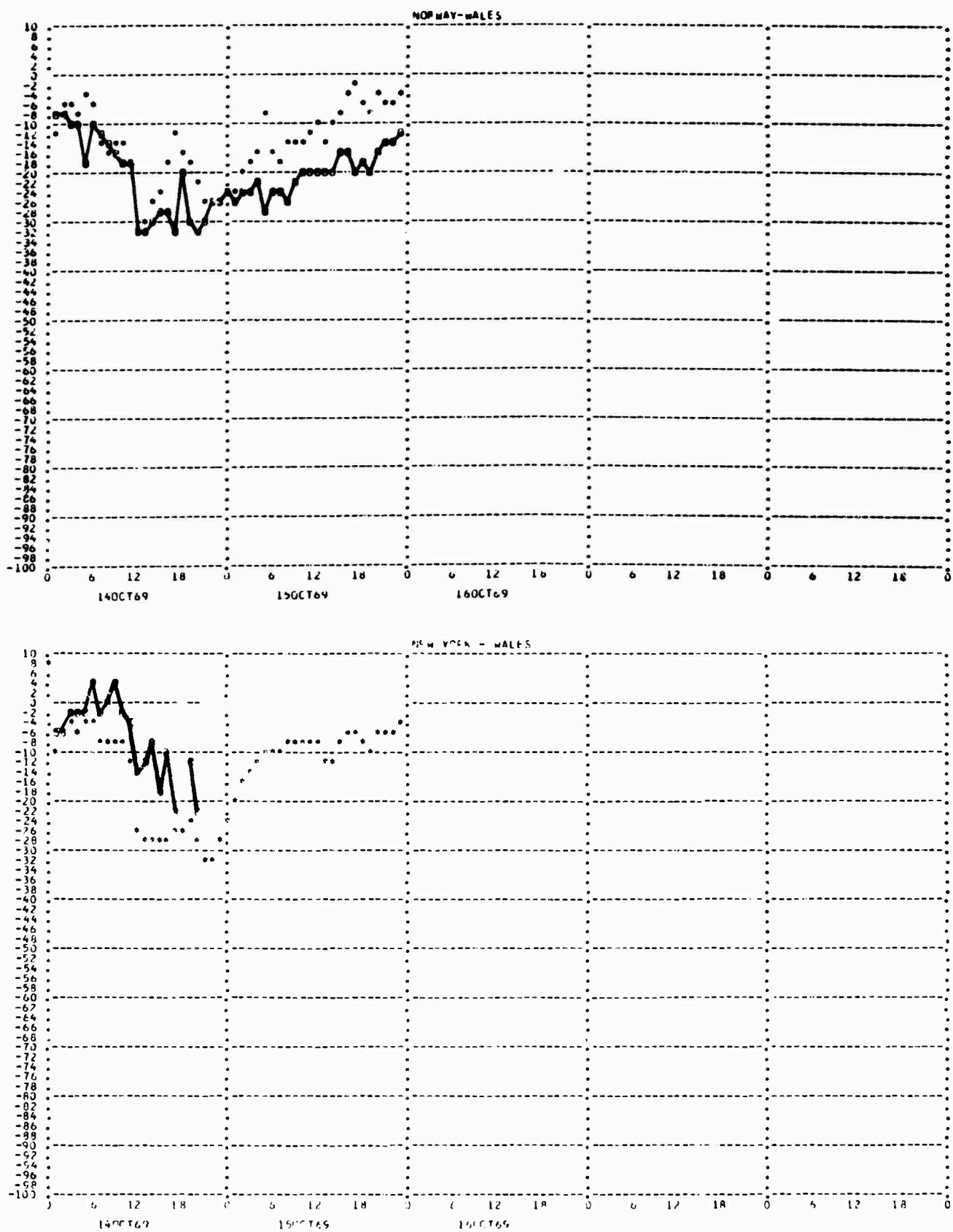


Figure 8. PCA events, 14 and 15 October 1969.

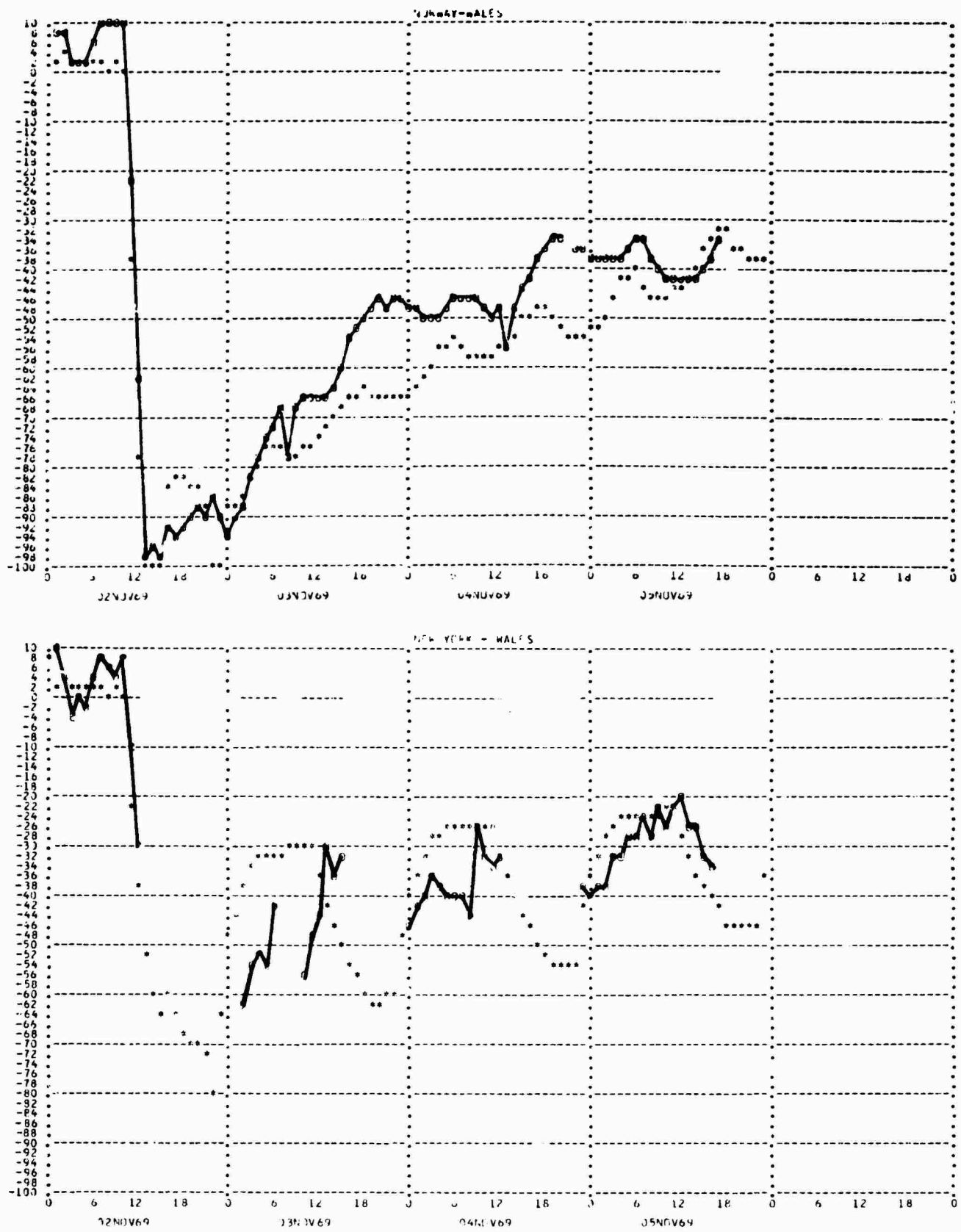


Figure 9. PCA events, 2, 3, 4 and 5 November 1969.

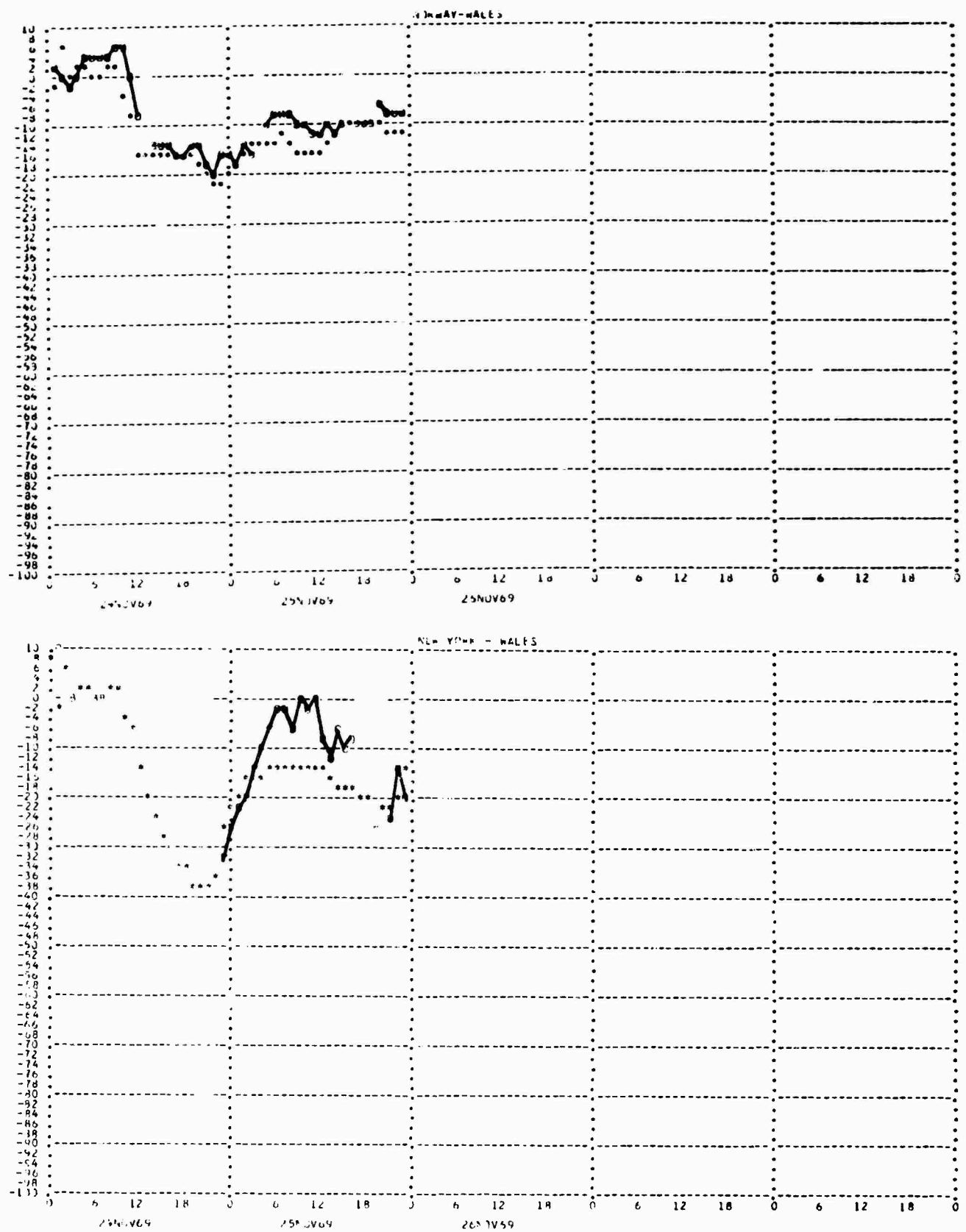


Figure 10. PCA events, 24 and 25 November 1969.

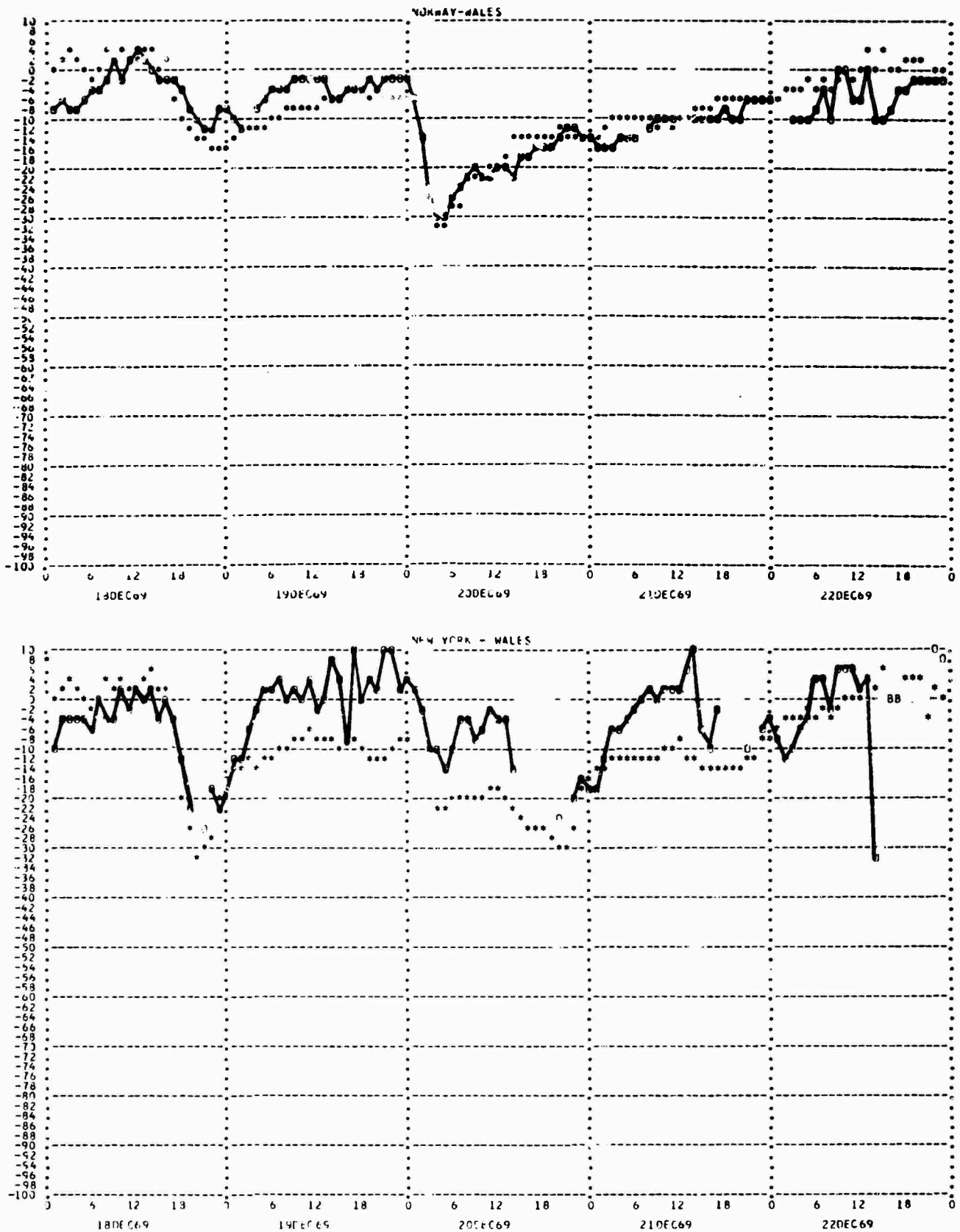


Figure 11. PCA events, 18, 19, 20, 21 and 22 December 1969.

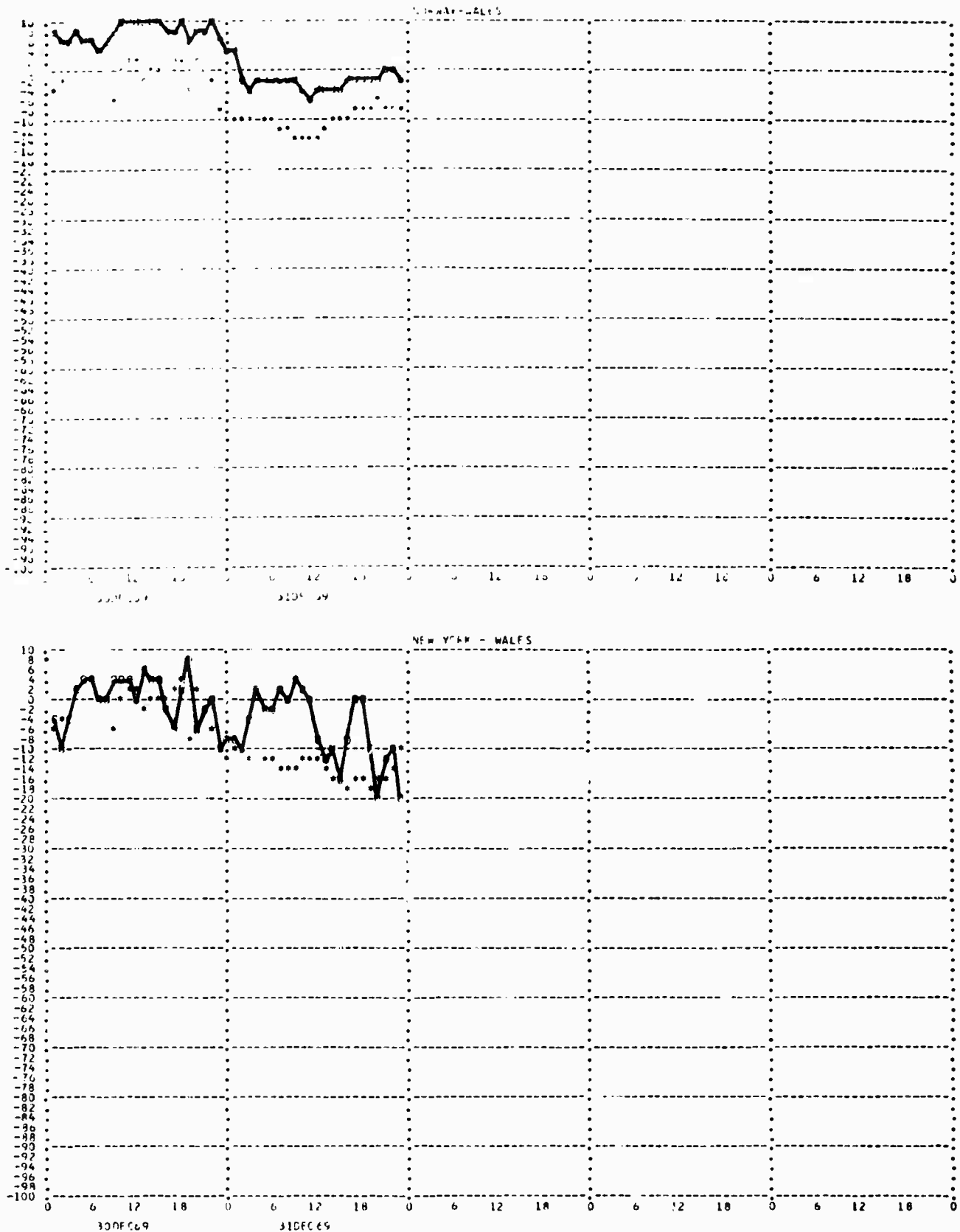


Figure 12. PCA events, 30 and 31 December 1969.

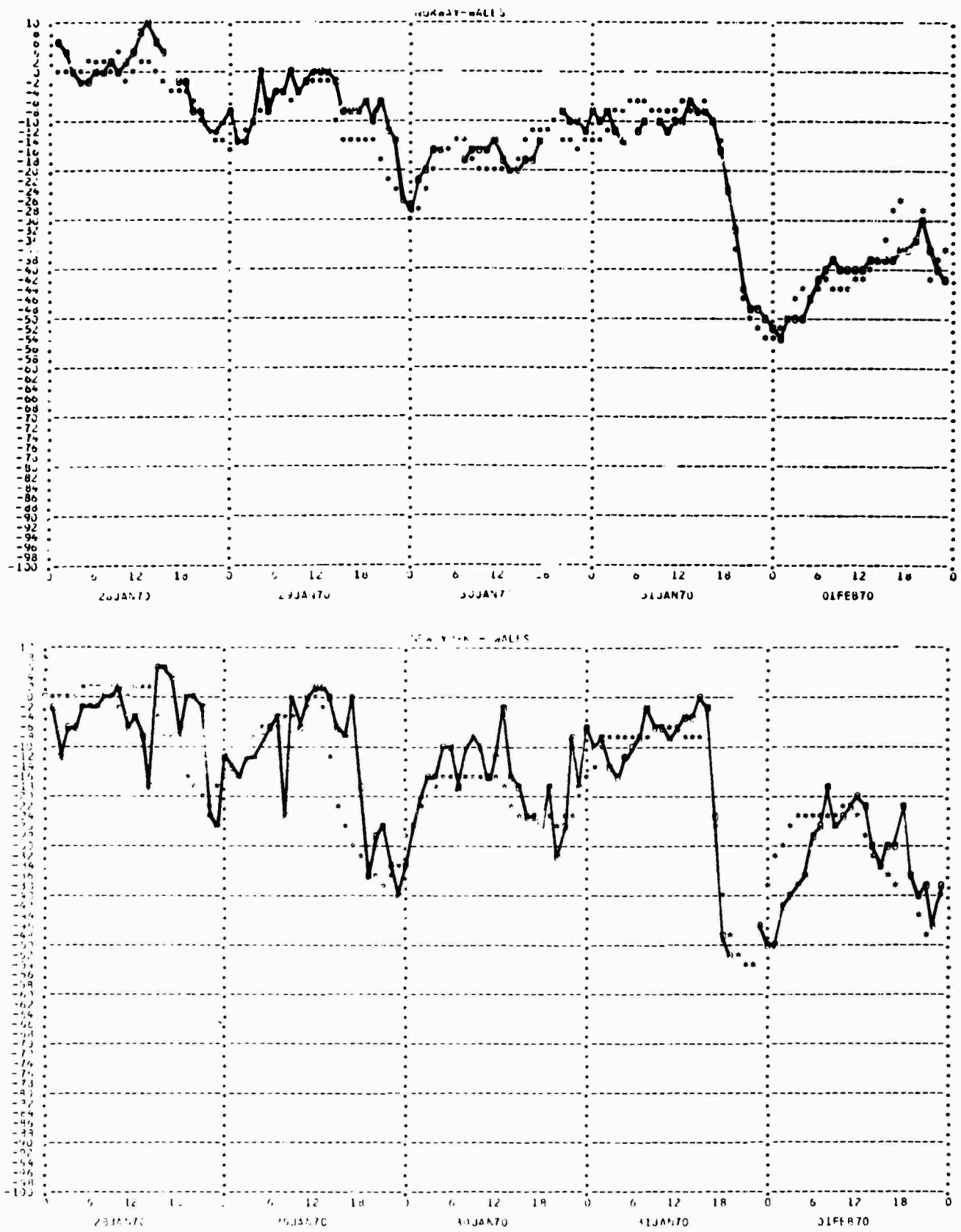


Figure 13. PCA events, 28, 29, 30 and 31 January 1970 and 1 February 1970.

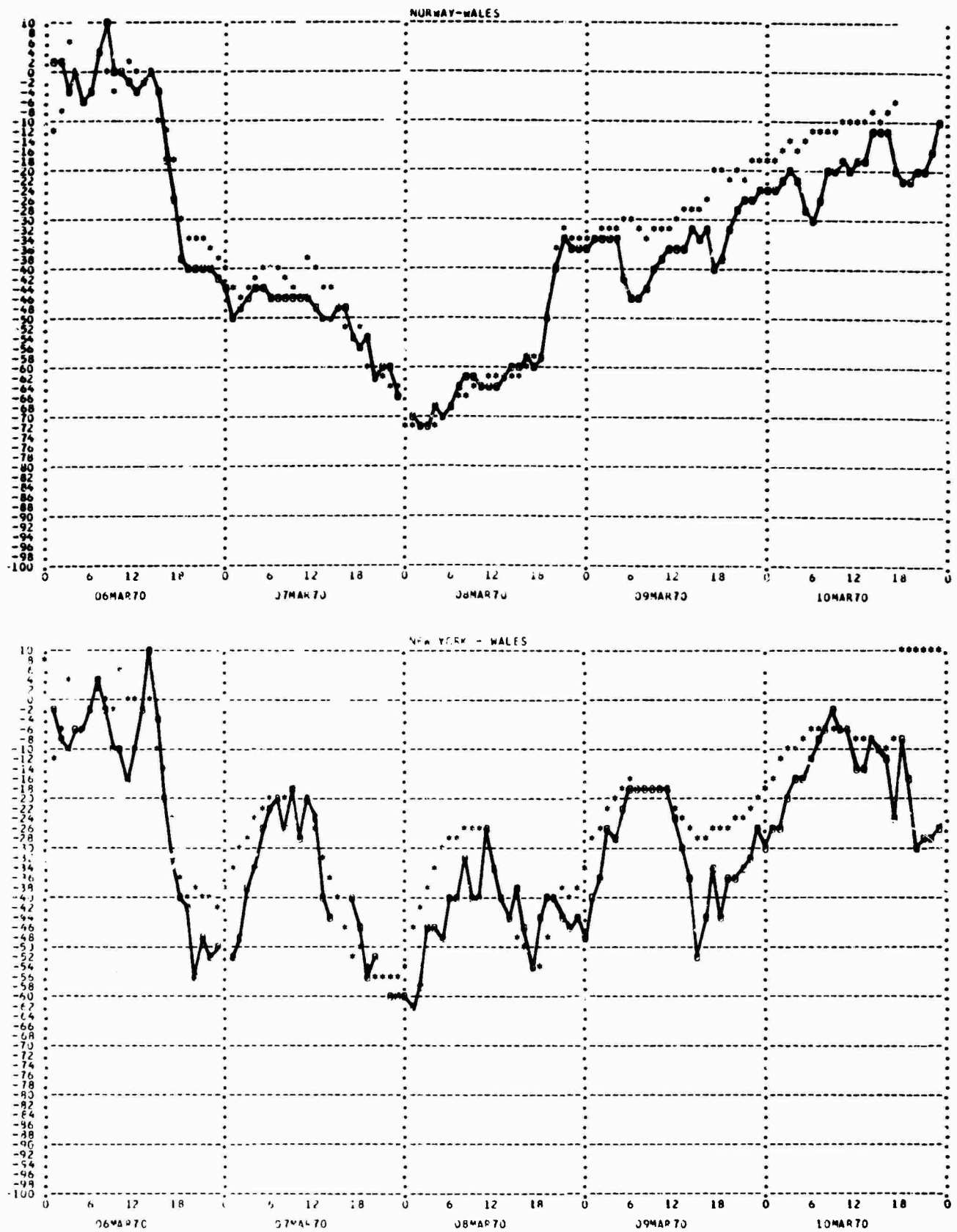


Figure 14. PCA events, 6, 7, 8, 9 and 10 March 1970.

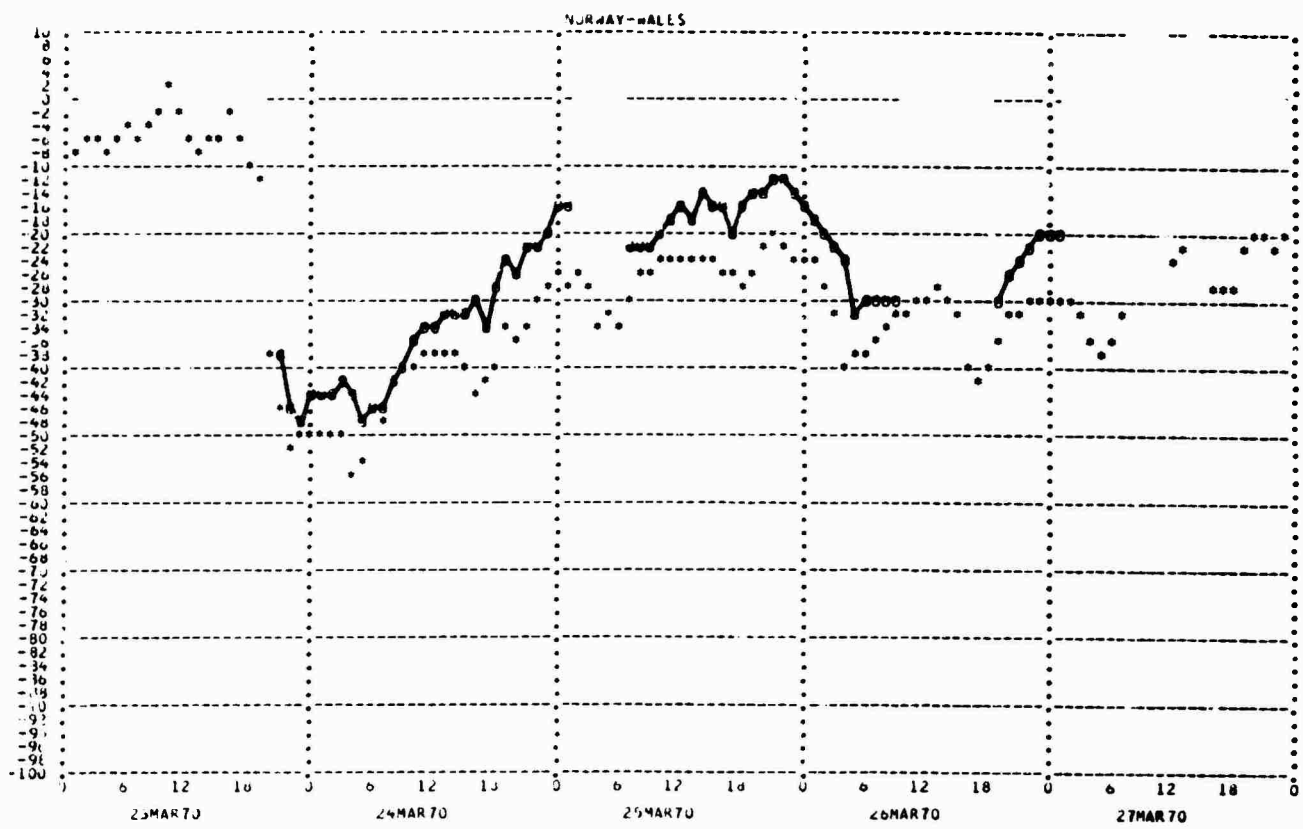


Figure 15. PCA events, 23, 24, 25, 26 and 27 March 1970.

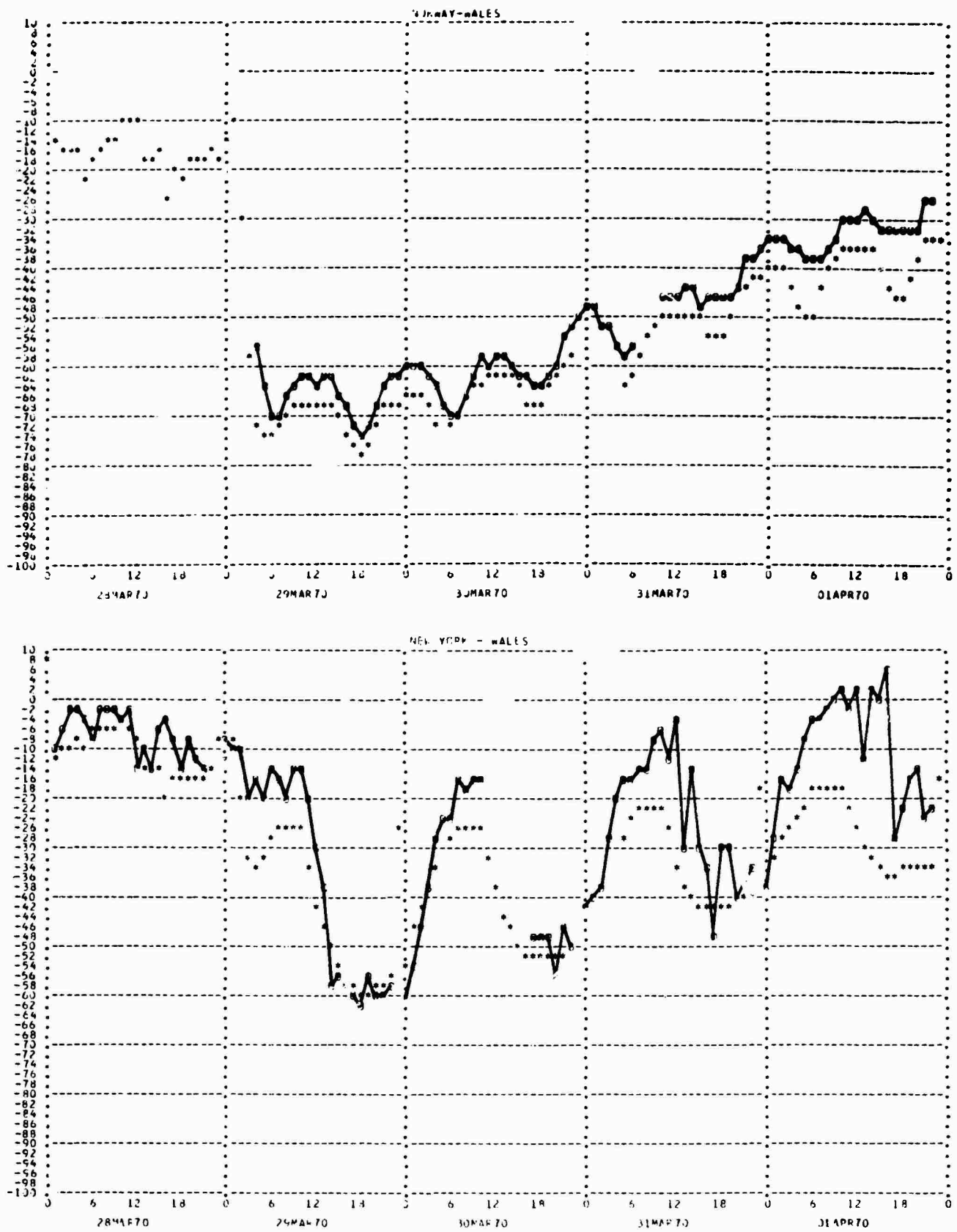


Figure 16. PCA events, 28, 29, 30 and 31 March 1970 and 1 April 1970.

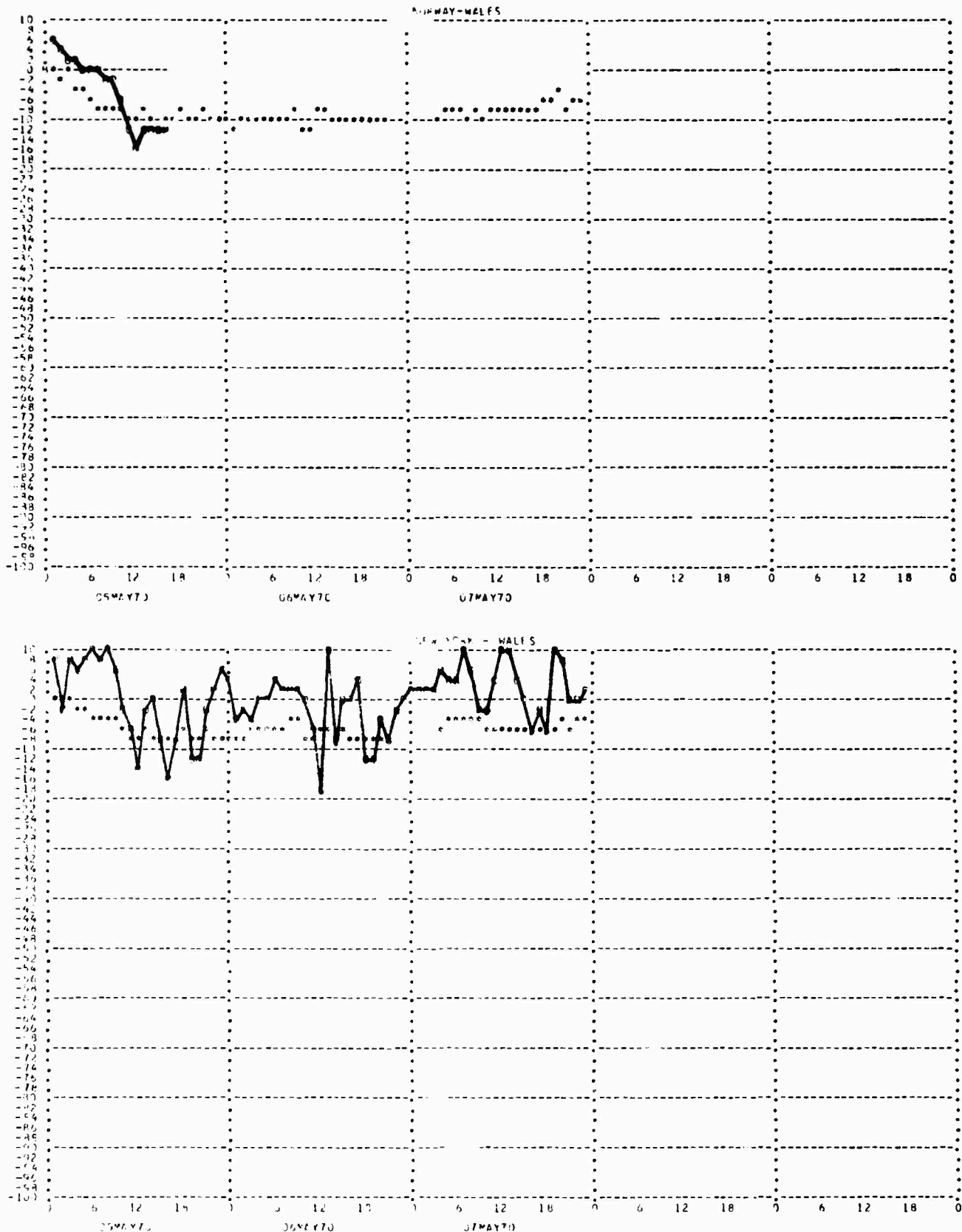


Figure 17. PCA events, 5, 6 and 7 May 1970.

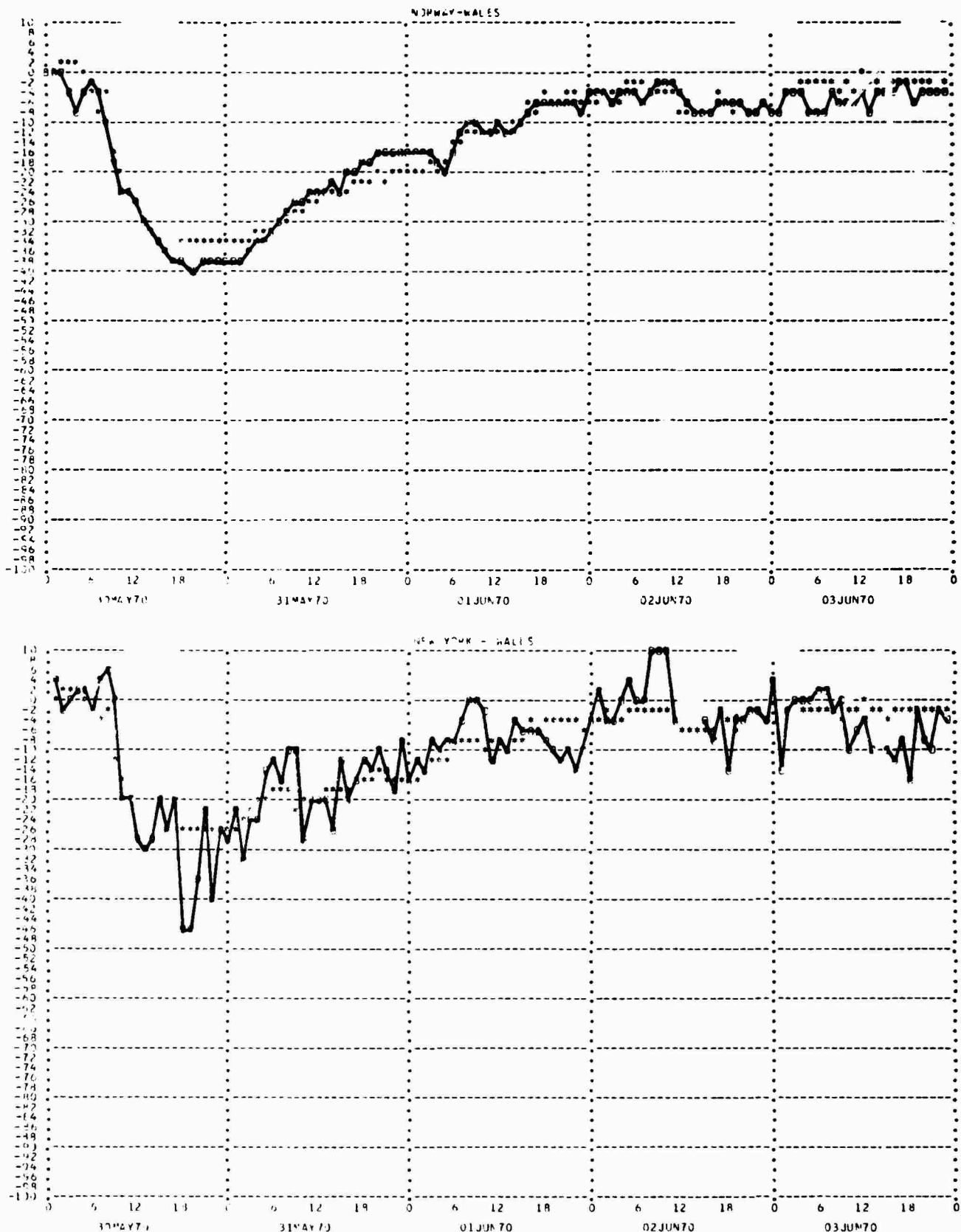


Figure 18. PCA events, 30 and 31 May 1970 and 1, 2 and 3 June 1970.

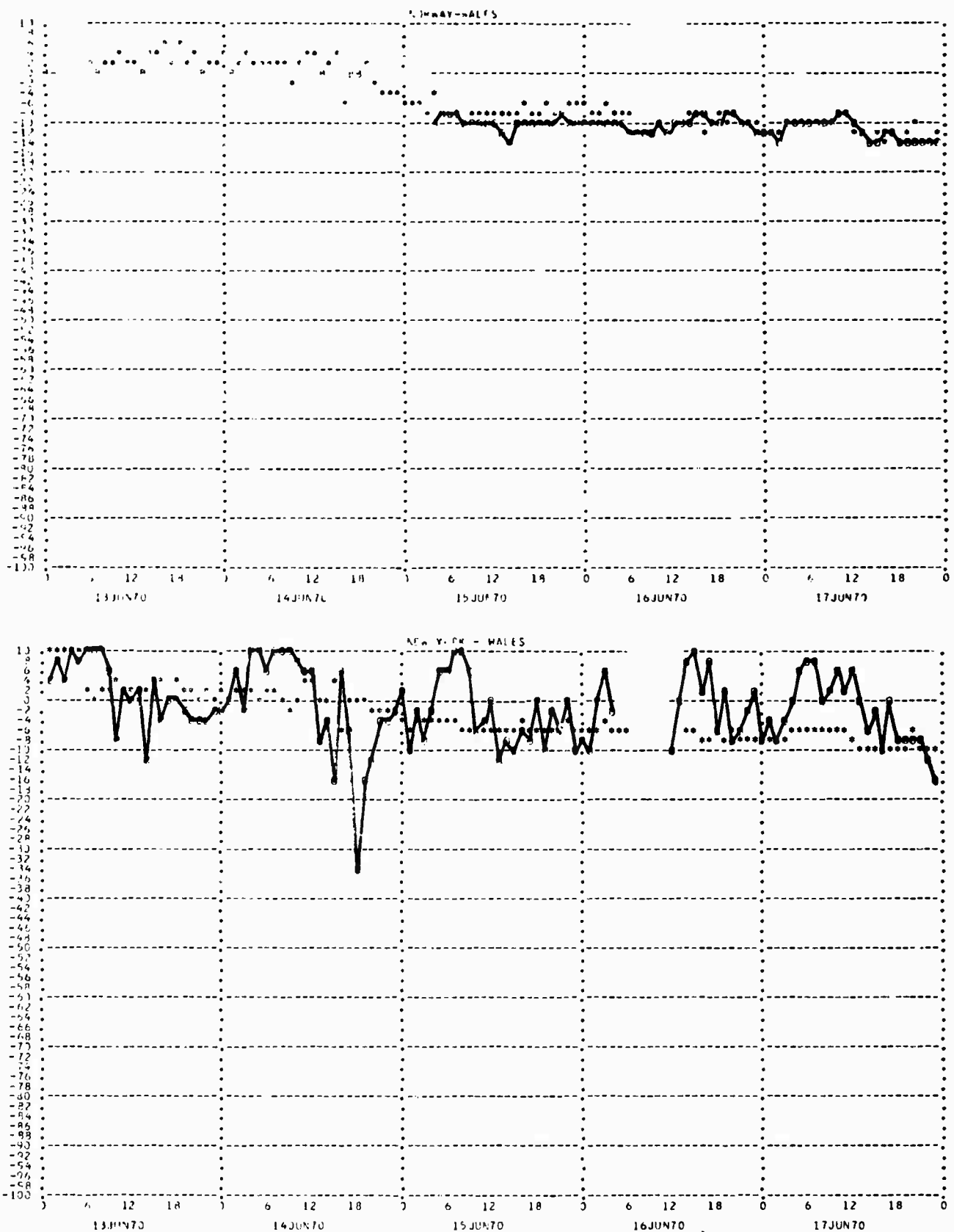


Figure 19. PCA events, 13, 14, 15, 16 and 17 June 1970.

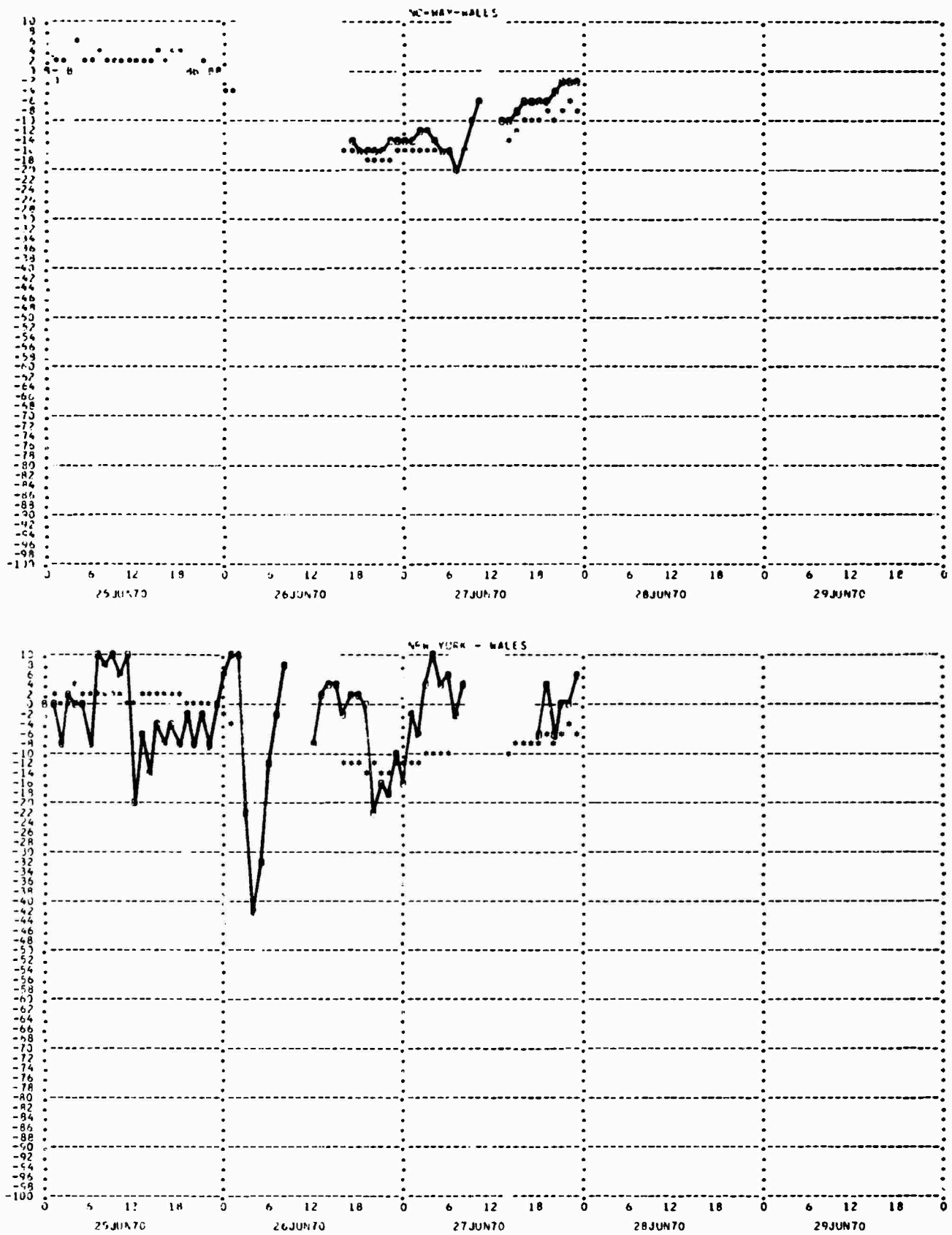


Figure 20. PCA events, 25, 26, 27, 28, and 29 June 1970.

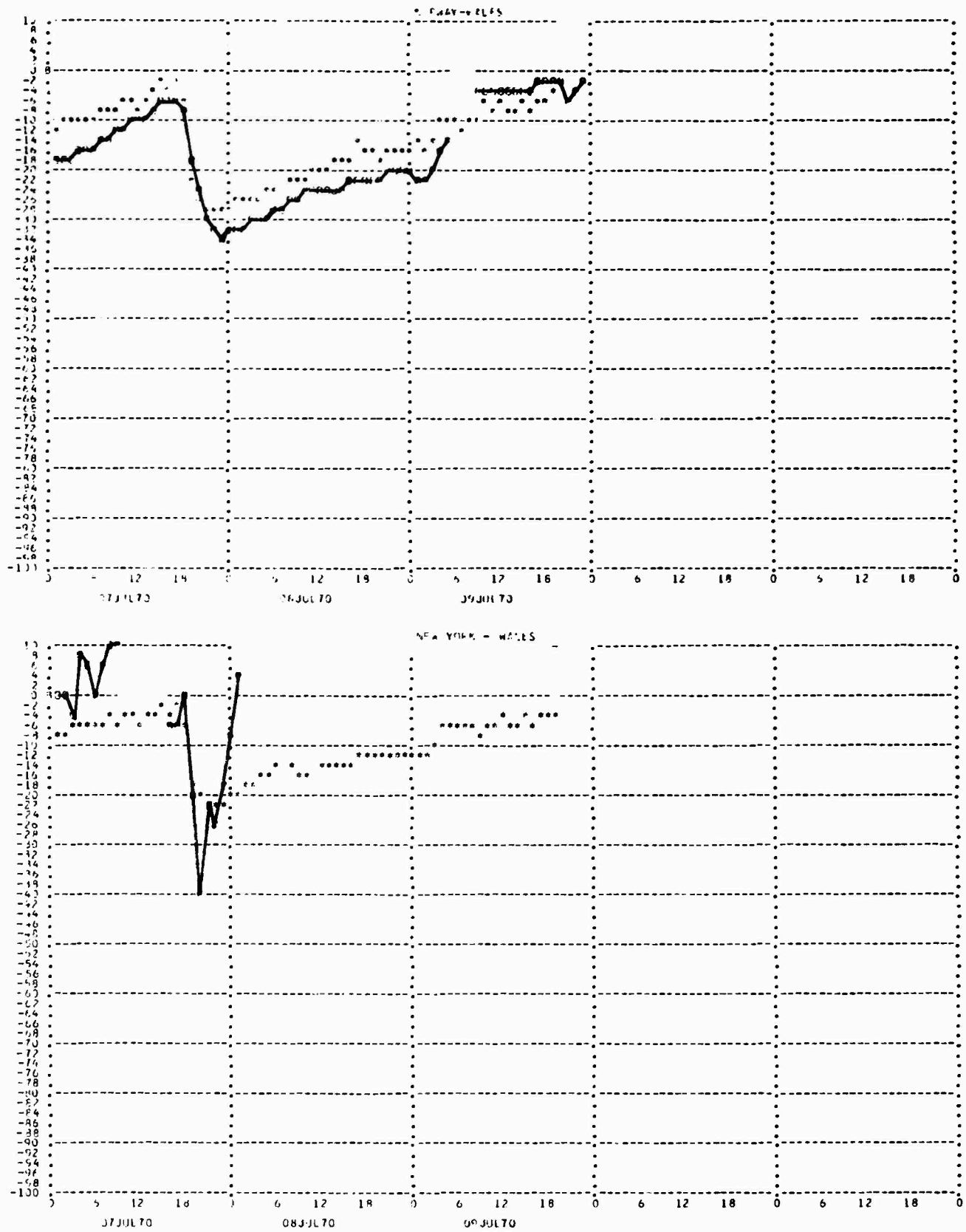


Figure 21. PCA events, 7, 8 and 9 July 1970.

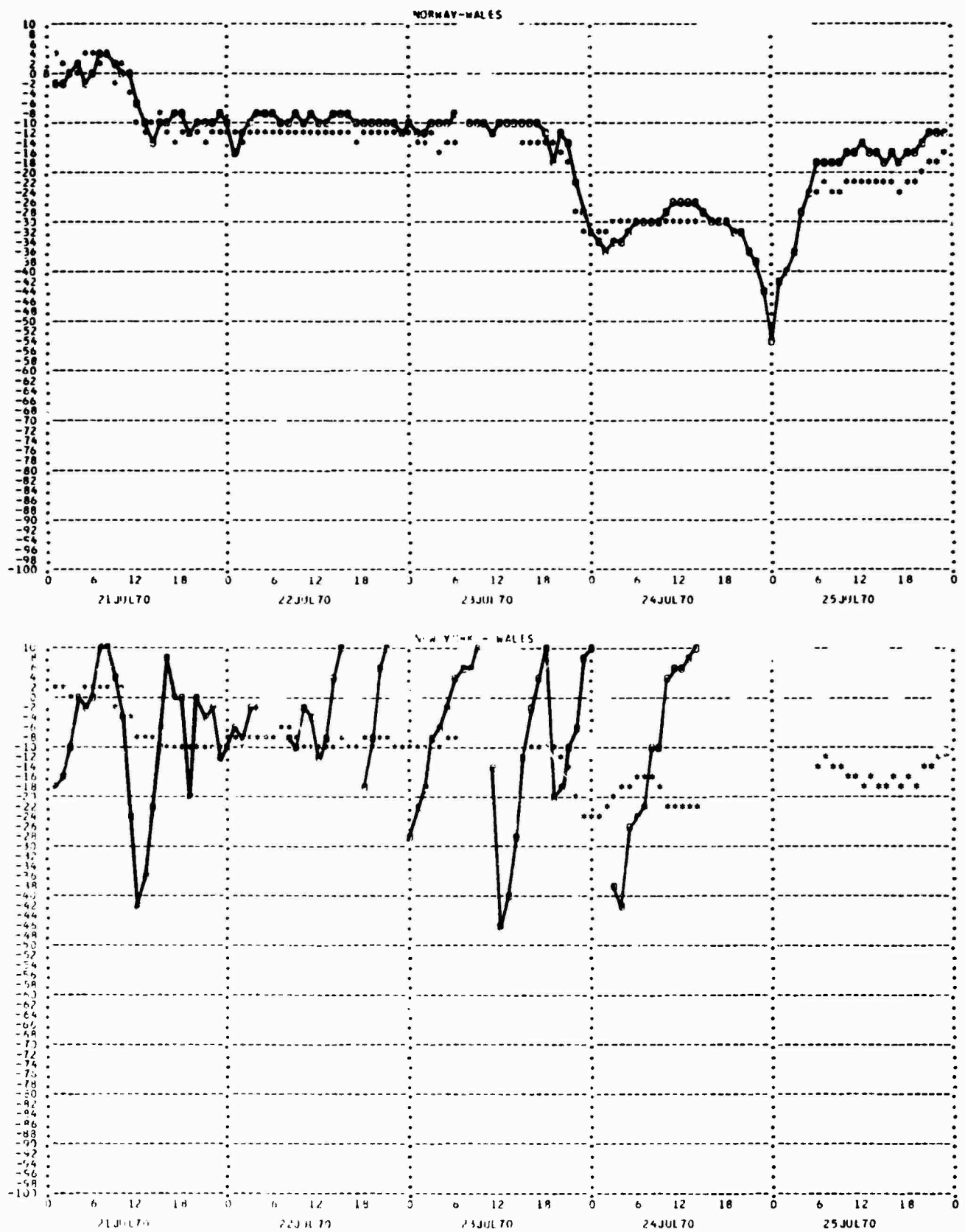


Figure 22. PCA events, 21, 22, 23, 24 and 25 July 1970.

an increase in the phase advance for the New York path (it is not completely within the "polar cap"). The SC occurred on 8 March 1970 and no anomalous phase advances took place at that time. The model does not predict the phase advance on the next day (9 March) which is seen on both paths. Since the Norway path lies completely within the polar cap, the cause is probably something other than expansion of the polar cap.

The data of 23 March 1970 on the New York path could not be reduced because of the large variations (not propagation-related) and so the second event, 28 March 1970 (which is really a continuation), is more completely shown. The late March period is on the boundary of the winter and summer models. Although the winter model (which was used) well explains the variations, the over predictions on the New York path on 1 April 1970 may be due to the onset of summer conditions.

The event of 30 May 1970 was the largest summer event in the data set. The scatter in the New York data increases later in the summer until PCA events are almost completely obscured. The signal strength of the New York path is marginally adequate under the best conditions (winter). Hence, during a summer event, the signal may be lost causing rapidly fluctuating phase data (as in the 21 July 1970 event).

Each of the events of 13 June, 25 June, and 07 July 1970 have spike phase advances at the onset of the PCA. These do not correlate with flares or SC's and are believed to be related to loss of signal strength.

## DISCUSSION

The data and models presented in the previous section indicate that, by knowing the general path conditions (diurnal sunlit patterns and the season) as well as the proton flux (energy greater than 10 MeV), the phase variations during a PCA event can be accurately evaluated.

To extend the phase-advance models to transpolar vlf propagation in general, the amount of the path which is affected (path length within the polar cap) must be determined. The structure of the disturbed D-region across the polar cap cannot be determined using data from two paths and, for this reason in this report, it is considered to be homogeneous. Future studies of PCA events and vlf phase advances should include measurements on more than just two paths because any variations in the altitude structure could have an impact upon the expected phase advances.

Martin<sup>5</sup> found that, generally, the Norway-to-Wales path has detectable phase advances more than one hour before those of the New York-to-Wales path. Martin's explanation is that the Norway to Wales path passes closer to the geomagnetic North Pole. This is in agreement with the Hakura<sup>6</sup> PCA model which states that the D-region electron density enhancements start at the pole and spread rapidly to the equatorial boundary. Thus, the Hakura model predicts that the Norway-to-Wales path has enhanced fluxes (phase advances) before the more southerly New York-to-Wales path. The model used in the study, which is the subject of this report, assumes a homogeneous proton flux caused enhancement over the entire polar cap and cannot, therefore, predict Martin's observations. The observed initial advances, however, were small (less than 10 centicycles) and, for this reason, do not constitute a major problem.

---

6. Hakura, K., "Entry of Solar Cosmic Rays Into the Polar Cap Atmosphere," Journal of Geophysical Research, Vol. 72, p. 1461, 1969

The accurate modeling of the vlf phase advances makes it possible to determine various aspects of the polar ionosphere such as the latitudinal extent of the polar cap and the altitude structure of the effective loss rate. Both of these factors are extremely important to the evaluation of the disturbance impact upon various ionospherically dependent systems.

It should be emphasized that single-mode propagation is assumed in all of the evaluations of data in this study. Previous phase advance models made no such assumptions. The NELC Waveguide computer program (which has been used successfully to model vlf multimode propagation in a highly accurate manner) was used to verify that, for these paths and frequencies, the propagation was single-mode dominated. These paths were approximately 5 000 kilometers in length over areas of poor conductivity (land). Over-water (good conductivity, sea-water) paths, even at the low frequencies used, will have multimode effects for up to 10 000 kilometers.

### LATITUDINAL EXTENT OF THE POLAR CAP

In the Hakura<sup>6</sup> model of PCA morphology, the initial enhanced D-region is above 65° corrected geomagnetic latitude (cgl). The expansion phase following a geomagnetic SC then pushes the enhancement to less than 60° cgl. The Norway to Alaska path is completely above 69° cgl and so lies almost completely within Hakura's polar cap. The New York-to-Alaska path, however, lies completely below 63° cgl and completely above 52° cgl as shown in figure 23. Thus, if the Hakura model (developed using hf riometers) was applicable to the vlf response to PCA events, the New York-to-Alaska path would remain unaffected until the expansion phase, at which time more than 60 percent of the New York-to-Alaska path would be affected.

The analysis and model of the fifteen events included in this study indicate that such is not the case. The New York-to-Alaska path is shown to be affected immediately and for the entire duration of the event.

Using the modeled variations, it is possible to calculate the extent of the vlf polar cap. The ratio of the normalized New York-to-Alaska variation to the normalized Norway-to-Alaska variation, together with figure 23, yields the latitude directly. The normalization should take into account the wavelength, the length of the path, and the propagation parameters (such as ground conductivity). Through the use of the NELC Waveguide program it was determined that the normalization was 0.95 percent. This means that, for a given reflection-height change of the polar D-region, the ratio of the changes will be approximately proportional to the ratio of the path lengths inside the polar cap.

Notice that  $\Delta\phi_{NY}/\Delta\phi_N = 1$  indicates that both paths are entirely inside the polar cap. The polar cap is at 56° cgl, approximately, when averaged over the diurnal variation, with an apparent midnight and noon value of 52° and 58° cgl, respectively. This hints at some slightly oval shape as indicated in figure 24.

The Norway-to-Alaska model on the New York-to-Alaska path, with a multiplying factor of 0.80 (corresponding to a circle of latitude 56° encompassing the changes), yields, however, almost exactly the same results in fitting the noisy New York to Alaska data ( $\delta = 10.7$  centicycles as opposed to  $\sigma = 10.7$  centicycles). Any attempts to obtain more information on the shape of the vlf polar cap will need significantly better (less noisy) data than was used in this study.

The indications are, therefore, that, using the proton flux and diurnal sunlit variations for a given path (as well as path lengths above 56° cgl), accurate predictions of the phase advances experienced by that propagation path will be possible.

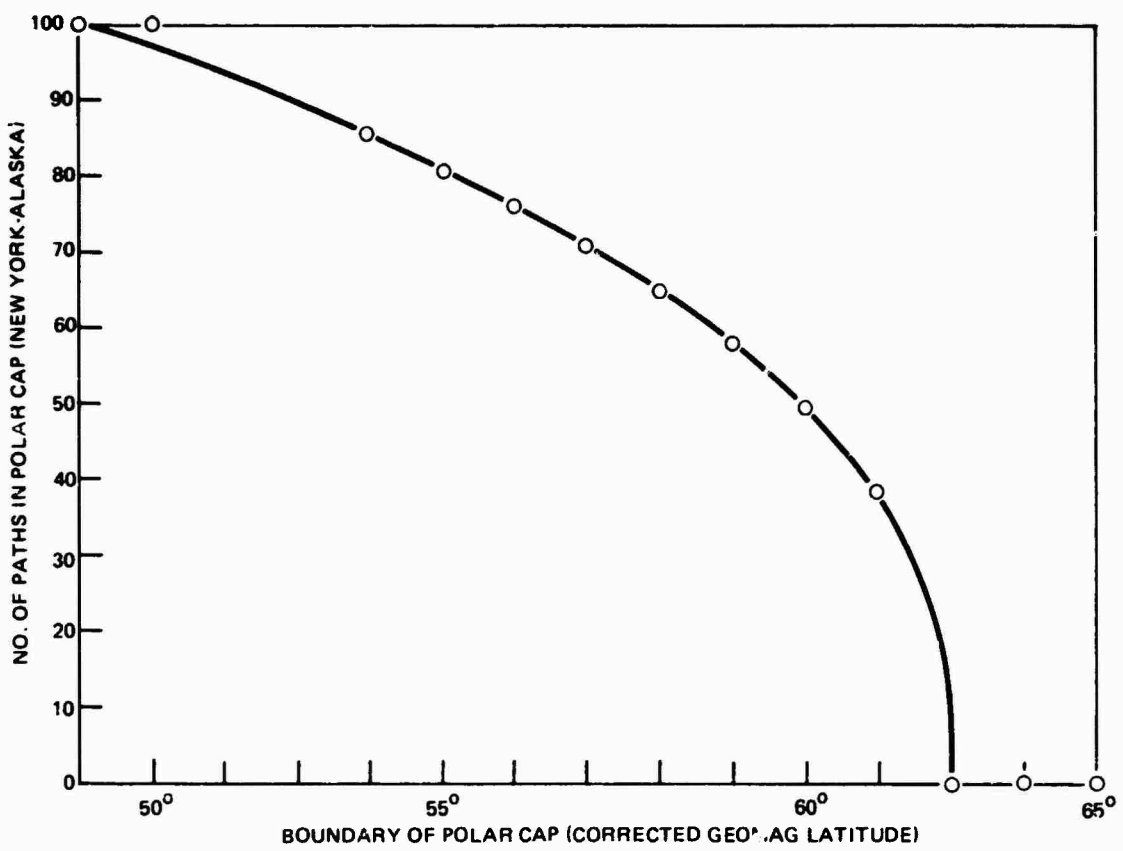


Figure 23. Corrected geomagnetic altitude, New York-to-Wales path.

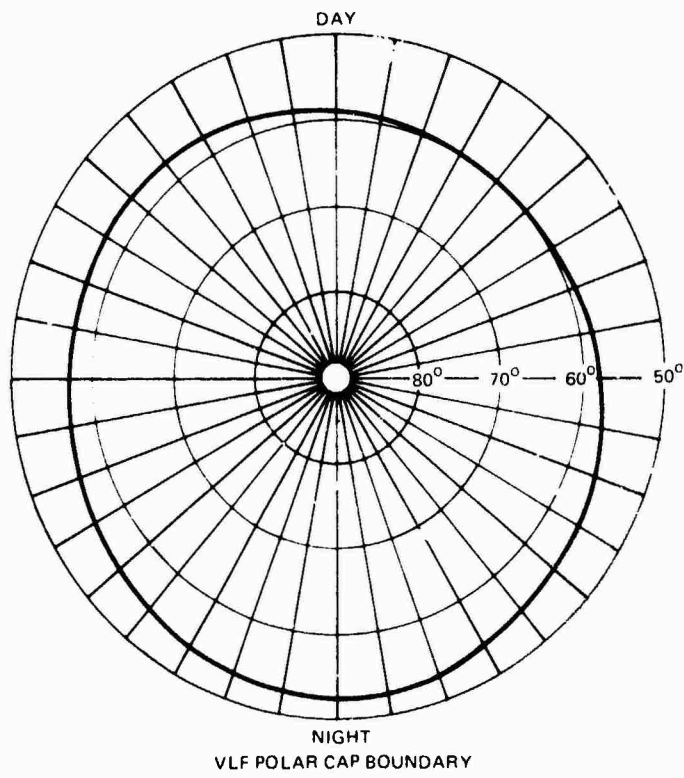


Figure 24. VLF polar cap boundary.

## DETERMINATION OF ALTITUDE STRUCTURE OF EFFECTIVE LOSS RATE

The modeled phase advances of the Norway-to-Alaska signal during these PCA events can be used to deduce the altitude structure of the disturbed D-region, effective steady-state loss rates ( $\psi$ ) for winter day and night conditions as well as for summer-day conditions.<sup>5</sup>

The effective loss rate is defined by the relationship  $Ne^2 = Q/\psi$  during steady-state conditions where  $Ne$  is the electron density and  $Q$  is the production rate. Thus, if the altitude structure of both  $Ne(h)$  and  $Q(h)$  is known,  $\psi(h)$  can be determined.

The ionization rate,  $Q(h)$ , has to be calculated using the method described by Argo<sup>7</sup> and can be approximated as being constant in altitude and directly proportional to flux (greater than 10 MeV) as shown in figure 25 ( $Q = 720 * \text{flux}$ ).

The electron density profile must be obtained by a more circuitous route. Using standard propagation models,<sup>8, 9</sup> the reflection height can be related to the measured phase advance as shown in figure 26 where single-mode theory is assumed.

Again assuming Wait's<sup>8</sup> model of an exponential ionosphere, the electron density at each reflection height is obtainable [ $Ne = 200 \exp(1.5*(70-h))$ ]. Hence, the reflection electron density and its altitude, shown in figure 27, are determined for each phase advance. Because the phase advance is a function of the proton flux (see figure 5), reflection electron density and altitude are uniquely determined for a given proton flux (as is the ionization  $Q(h)$ ). Hence, by using various flux values,  $Ne^2(h)/Q(h)$  can be calculated, yielding the  $\psi(h)$ 's in figure 28, for various conditions (day/night, seasonal).

The loss-rate values determined by this method agree with the monotonically decreasing-with-increasing-altitude quiet-time loss rates given by Poppoff.<sup>10</sup> This differs from the conclusion of Montbriand and Belrose<sup>3</sup> that the loss rate increases (with increasing altitude) between 60 and 80 kilometers.

A definite seasonal variation is indicated by the data. The summer loss rates below 70 kilometers are several times larger than the winter loss rates. Larsen<sup>4</sup> postulates that the seasonal effect would be due to the cold summer mesosphere allowing a larger degree of hydration. This then would lead directly to larger values of the electron-ion dissociative recombination rate coefficient, which constitutes part of  $\psi$ .

---

7. Argo, P. E., Electron Production Rate of Solar and Galactic Cosmic Rays in the Lower Ionosphere D-Region, NELC TR 1783, 11 August 1971

8. Wait, J. R., and K. P. Spies, Characteristics of the Earth's Ionospheric Waveguide for VLF Radio Waves, NBS TN 300.

9. Davies, K., Ionospheric Radio Propagation, NBS Monograph 30, 1 April 1964.

10. Poppoff, I. G., R. C. Whitten, R. C. Gunton, J. E. Evans, and E. G. Jolci, "Data-Gathering Methods Based on Atmospheric Measurements," Defense Nuclear Agency Reaction Rate Handbook, Report 1948H, March 1972.

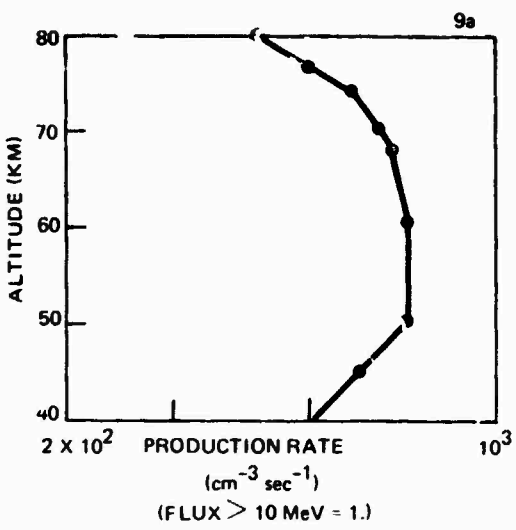


Figure 25. Ionization Rate.

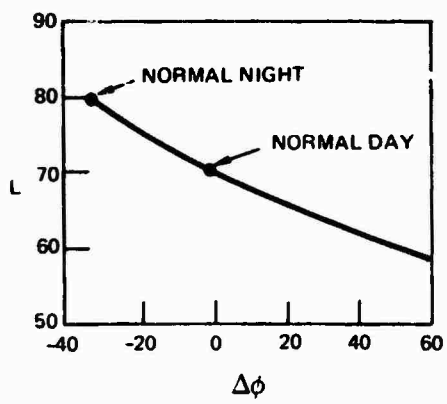


Figure 26. Measured phase advance.

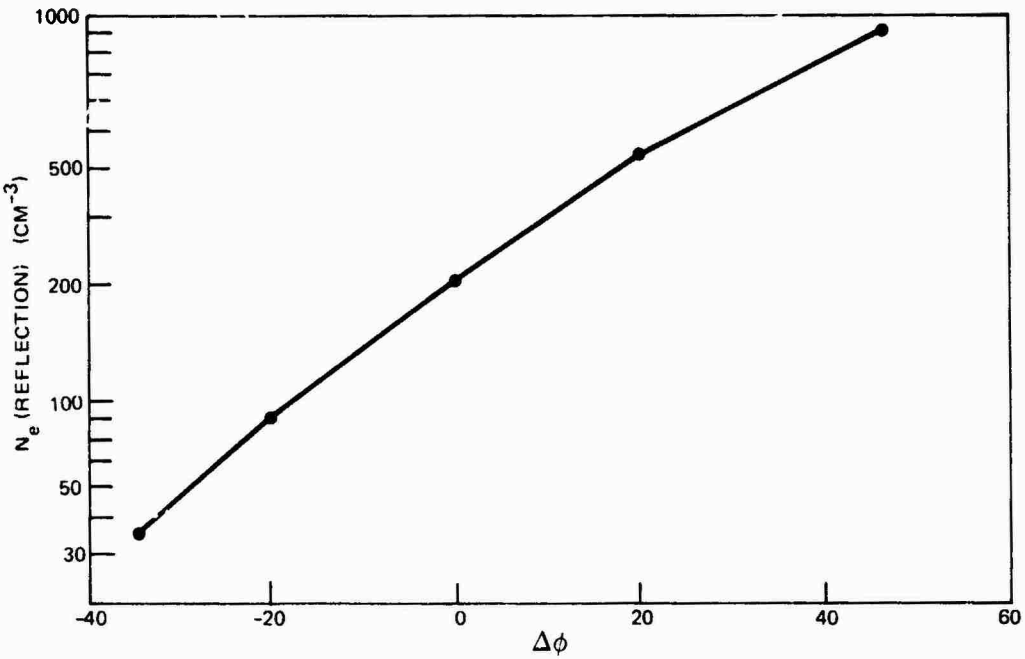


Figure 27. Reflected electron density.

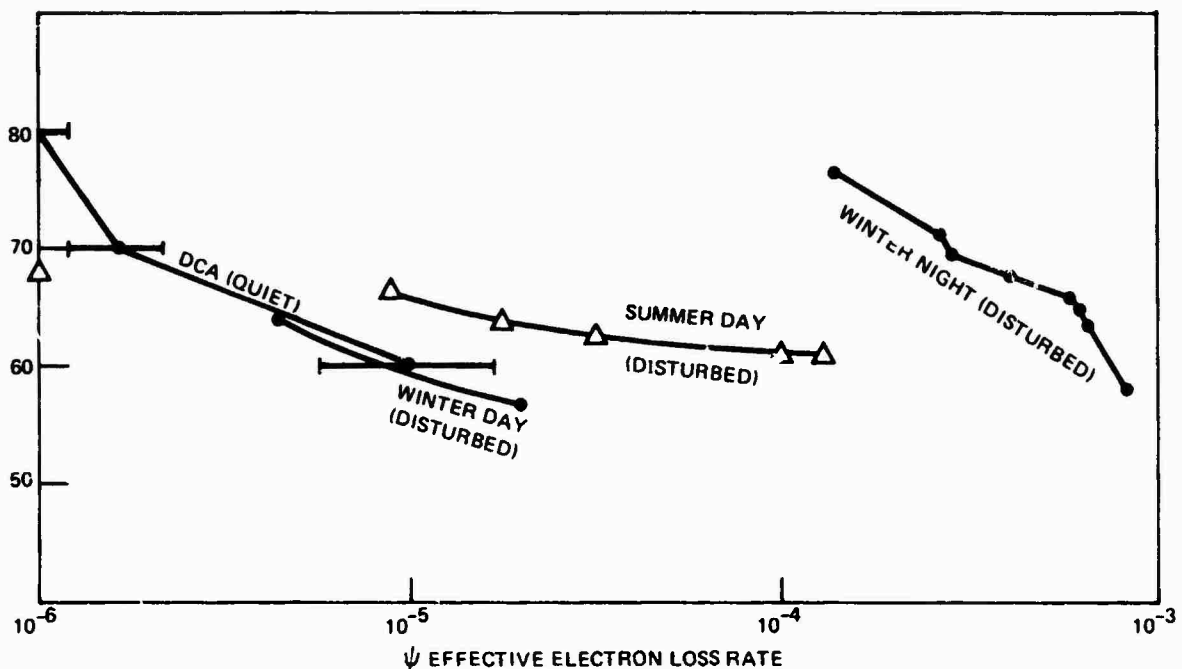


Figure 28. Effective electron-loss rate.

## SUMMARY

The effects upon vlf navigational systems due to ionospheric changes caused by solar proton events (i.e. PCAs) can be accurately estimated using only the geophysical conditions along the path (amount of path in sunlight, path length above  $56^\circ$  corrected geomagnetic latitude, and season) and the instantaneous proton flux (as measured by a satellite such as SOLRAD XI). These estimates can reduce navigational errors to within one nautical mile.

An important outcome of this study is the discovery that the "vlf polar cap" extends to  $\approx 56^\circ$  which is seven degrees nearer to the equator than the  $63^\circ$  normally used. In fact, this large polar cap is at the previous "worst-case" latitude which was thought to occur in the late stages of Hakura's PCA model.

This vlf polar cap, which is the polar region in which vlf signals undergo phase advances caused by solar proton events, differs from the polar cap which is usually defined as the region toward the pole from the auroral oval. This larger measure of the polar cap does not imply that the auroral oval is extended in the direction of the equator from the vlf polar cap. The large size of the polar cap in relation to vlf signals probably results from the fact that vlf propagation is affected at lower altitudes than are riometers, and the higher energy particles doing the ionizing have lower cutoff latitudes. The fact that the polar cap extends seven degrees greater than previous measurements<sup>6</sup> in the direction of the equator is extremely important to global vlf navigational systems such as Omega because the area affected during a PCA event is much greater than just the polar cap itself.

In fact, any location having at least one propagation path (to an Omega transmitting station) that passes within the polar cap, will cause position errors if it uses the transpolar path. Large portions of the earth's surface receive only one non-transpolar signal. These regions clearly must be affected by any PCA event. Figures 29 and 30 show the affected areas for the present and future Omega configuration, while figure 31 indicates the before and after positioning errors during a relatively severe event. Notice that the affected region (the Atlantic Ocean) is extremely important to all Department of Defense users. It would appear extremely important, therefore, to implement the phase corrections as described in this report.

The two propagation paths used in this study allow an estimate to be made of the extent of the polar cap. More paths would enable a study of the polar D-Region structure and would provide an answer to the question of whether there is an extra enhanced D-Region corresponding to the auroral oval. This structure would be very important to paths crossing the low-latitude extremities of the polar cap and knowledge of it would lead to increased navigational accuracy.

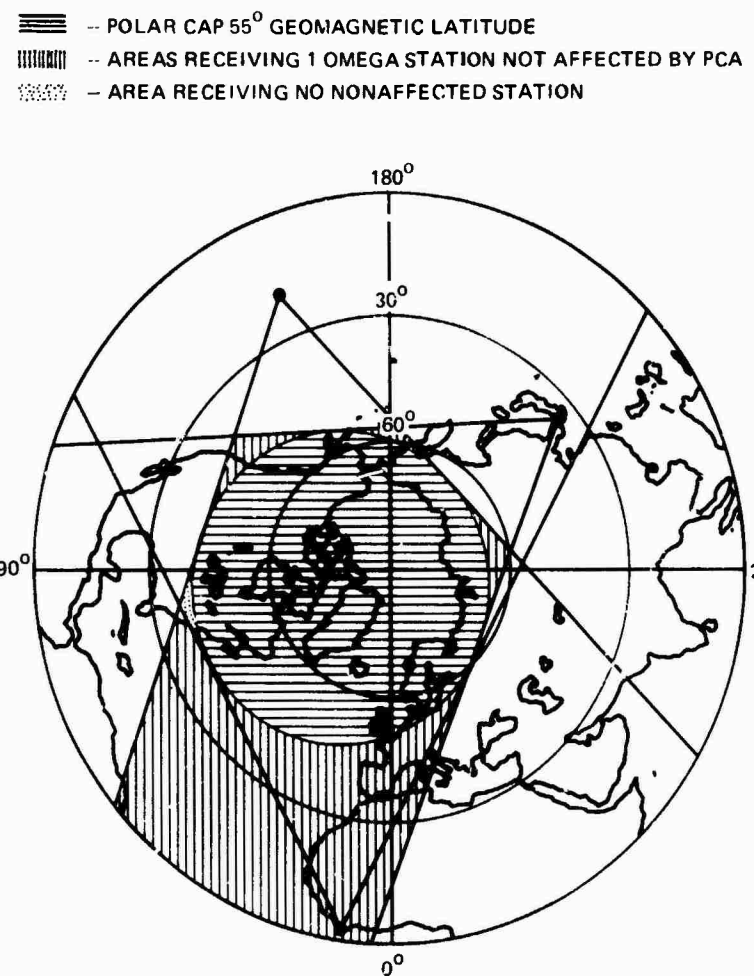


Figure 29. PCA event using Liberian station.


 - POLAR CAP 55° GEOMAGNETIC LATITUDE  
 - AREAS RECEIVING 1 OMEGA STATION NOT AFFECTED BY PCA  
 - AREA RECEIVING NO NONAFFECTION STATION

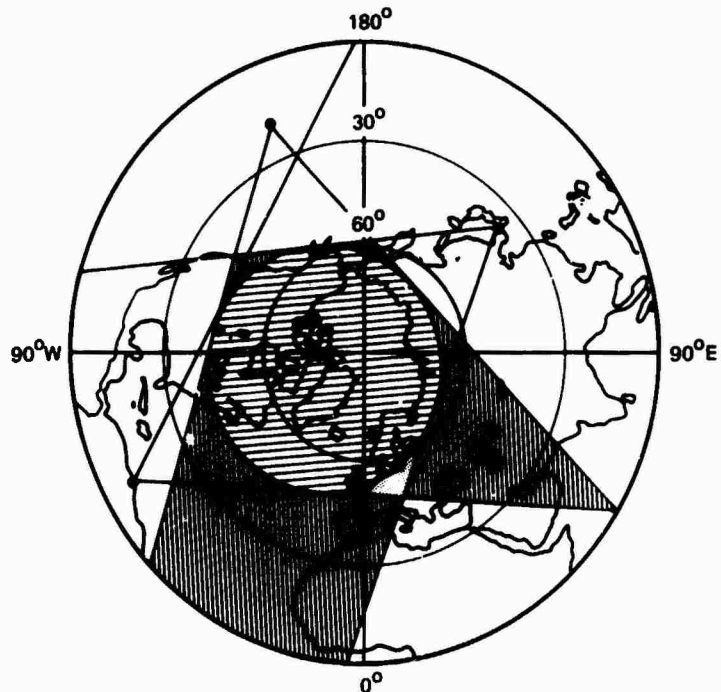


Figure 30. PCA event using Trinidad station.

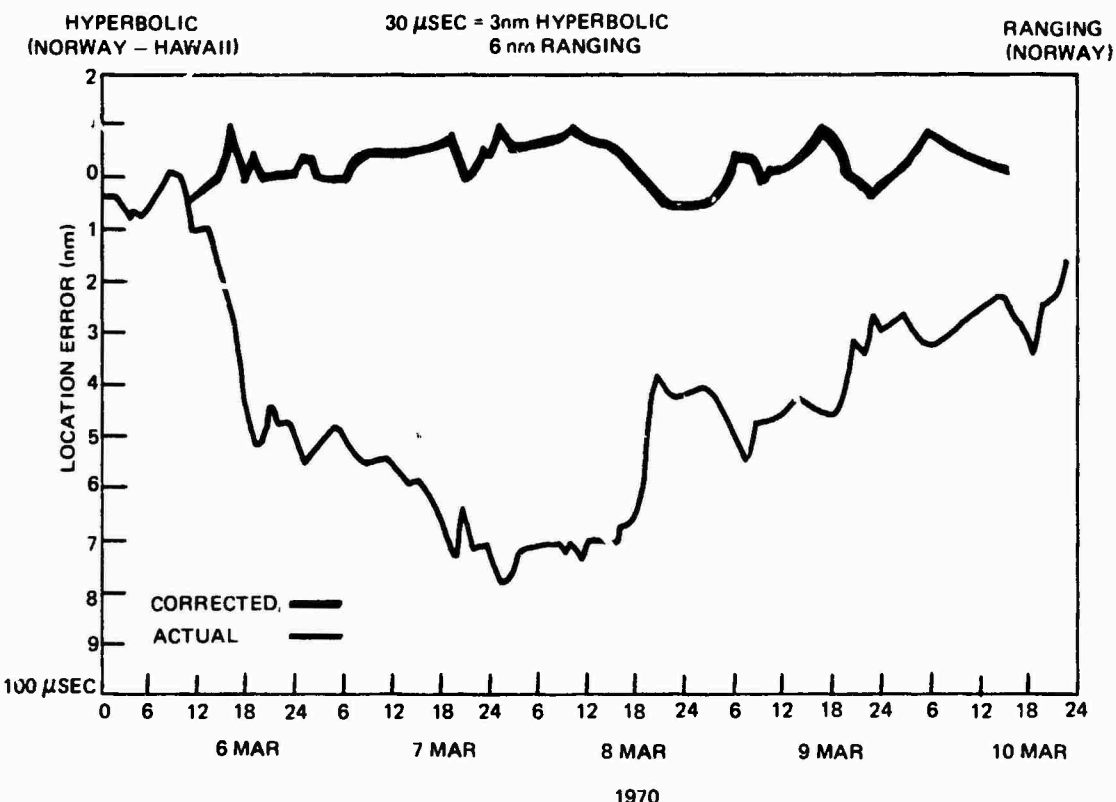


Figure 31. Before and after positioning errors during a severe event.

## REFERENCES

1. Westerlund, S., F. H. Rader, and C. Asom, "Effects of Polar Cap Absorption Events on VLF Transmissions," Planet, Space Science, Vol. 17, p. 1329, 1969.
2. Martin, J. N., Omega Phase Variations During PCA Events, NELC TR 1835, 17 August 1972.
3. Montbriand, L. E., and J. S. Belrose, "Effective Electron Loss Rates in the Lower D-Region During the Decay of Solar X-Ray Events," Radio Science, Vol. 7, No. 1, p. 133-172, 1972.
4. Larsen, T. R., Disturbances in the High-Latitude Lower Ionosphere, NDRE Report No. 62, Norwegian Defense Research Establishment, March 1973.
5. Argo, P. E. and I. J. Rothmuller, Effective Electron Loss Rates in the Polar D-Region During Polar Cap Absorption Events, NELC TN 2890, 18 February 1975.
6. Hakura, K., "Entry of Solar Cosmic Rays into the Polar Cap Atmosphere," Journal of Geophysical Research, Vol. 72, p. 1461, 1967.
7. Argo, P. E., Electron Production Rate of Solar and Galactic Cosmic Rays in the Lower Ionosphere D-Region, NELC TR 1783, 11 August 1971.
8. Wait, J. R., and K. P. Spies, Characteristics of the Earth's Ionospheric Waveguide for VLF Radio Waves, NBS TN 300.
9. Davies, K., Ionospheric Radio Propagation, NBS Monograph 80, 1 April 1964.
10. Poppoff, I. G., R. C. Whitten, R. C. Gunton, J. E. Evans, and E. G. Jolci, "Data-Gathering Methods Based on Atmospheric Measurements," Defense Nuclear Agency Reaction Rate Handbook, Report 19848H, March 1972.